

Configuration Models of Random Hypergraphs and Their Applications

Philip S. Chodrow*

*Operations Research Center
Laboratory for Information and Decision Systems
Massachusetts Institute of Technology*

November 8, 2021

Abstract

Networks of dyadic relationships between entities have emerged as a dominant paradigm for modeling complex systems. Many empirical “networks” – such as collaboration networks; co-occurrence networks; and communication networks – are intrinsically polyadic, with multiple entities interacting simultaneously. Historically, such polyadic data has been represented dyadically via a standard projection operation. While convenient, this projection often has unintended and uncontrolled impact on downstream analysis, especially null hypothesis-testing. In this work, we develop a class of random null models for polyadic data in the framework of hypergraphs, therefore circumventing the need for projection. The null models we define are uniform on the space of hypergraphs sharing common degree and edge dimension sequences, and thus provide direct generalizations of the classical configuration model of network science. We also Metropolis-Hastings algorithms in order to sample from these spaces. We then apply the model to study two classical network topics – clustering and assortativity – as well as one contemporary, polyadic topic – simplicial closure. In each application, we emphasize the importance of randomizing over hypergraph space rather than projected graph space, showing that this choice can dramatically alter directional study conclusions and statistical findings. For example, we find that many of social networks we study are *less* clustered than would be expected at random, a finding in tension with much conventional wisdom within network science. Our findings underscore the importance of carefully choosing appropriate null spaces for polyadic relational data, and demonstrate the utility of random hypergraphs in many study contexts.

1 Introduction

A complex systems consists of a set of entities joined by relationships. Familiar examples from social and information networks include agents bound by social interactions; [1, 2]; colleagues joined by collaborations [3, 4, 5, 6, 7] or correspondences [8]; and compositions of food in recipes, tags on posts, or classifications on patents [9, 10]. In each of these examples, relationships are natively polyadic: arbitrary numbers of entities able to interact

*pchodrow@mit.edu

simultaneously. Over the last two decades, the dominant approach to such systems has been to represent them via dyadic network modeling, which allows relationships between two entities at a time. Typically, a polyadic relationship between k entities is represented by a total of $\binom{k}{2}$ dyadic relationships, one for each pair of the k entities, resulting in the *projected graph* of the system. This paradigm has enjoyed striking success over the last two decades, leading to computationally tractable and scientifically insightful models.

Recent work, however, has highlighted limitations of the dyadic paradigm in description, inference, and prediction of properties of complex systems. Developments in network neuroscience, for example, have underscored the need to model polyadic relationships to describe both temporal and structural connections between functional units of the brain [11]. Studies of ecological [12] and social [13] dynamics have demonstrated time-dependent behaviors that cannot be reproduced under parsimonious pairwise models. “Higher-order” (polyadic) structures have been found to be useful in describing, inferring, and predicting structural properties of many networked data sets [9, 14, 15].

Recent interest has therefore turned to the development of natively polyadic representations and measurements for relational data. In many cases, interpretations of these measurements require comparison against a statistical *null model*. The purpose of such a model is to control for “uninteresting” features of the data. The model can then tell us whether an observed measurement is probabilistically consistent with the “uninteresting” features. If not, the measurement may suggest the presence of additional features in the data over and above what we have controlled for. Null models are an integral part of the scientific treatment of data, and implicitly underscore all judgments of “statistical significance” in scientific data analysis. Null models of dyadic networks have traditionally taken the form of random graphs – probability distributions over a space of graphs chosen to be in some sense comparable to the data. The most important null model of the previous two decades is the *configuration model* in which the network is randomized while preserving the number of neighbors of each node [16, 17].

The importance of polyadic networks and the success of the dyadic configuration model naturally suggest that the latter be generalized to treat the former. Unfortunately, in contrast to the relatively mature state of dyadic random graph theory, random null models for polyadic networks are still in their infancy. There are by now a handful of random polyadic structures purpose-built for various analytical tasks [18, 19, 20, 21, 22, 23, 24]. As we will argue below, however, none fully inherit the flexibility and generality of the dyadic configuration model.

Outline of the Paper

The purpose of this work is to develop a flexible null model for polyadic data that maintains as many properties as possible of the dyadic configuration model. While this problem is of intrinsic mathematical interest, we are primarily motivated by applications to exploratory, inferential, and predictive analysis in polyadic network data science. We begin in Section 2 with a review of the landscape of null models for relational data sets, including the (dyadic) network configuration model, random hypergraphs, and random simplicial complexes. Along the way, we introduce two points that guide much of our subsequent development. First, the mode in which we *represent* data (e.g. as graphs, hypergraphs, or simplicial complexes) determines what we are able to reliably *measure*. For example, representations that discard or modify degree information will distort measures of degree-assortativity. Notably, both projected dyadic graphs and simplicial complexes fall into this category. Second, a mode of

data representation is implicitly a choice of space over which we randomize. Because of this, the choice to randomize before or after transforming data can have large enough impact to drive contradictory study findings. We argue for randomizing prior to transformations, and the remainder of the paper may be viewed as a recipe for how to do this. In Section 3, we define a configuration model for random hypergraphs, including stub-labeled and vertex-labeled variants [25]. This model preserves both the degree and edge-dimension distributions of the original data set, and therefore accounts for all “zeroth-order” information about the data. Application of the model requires a sampling scheme, which we provide in Section 4.

We turn to a triplet of applications in Section 5. In Section 5.1, we study triadic closure. Comparison against dyadic configuration models generally suggests that empirical social networks display much higher rates of triadic closure than would be expected by chance. We argue instead for the application of our hypergraph configuration model, and through it find that most of our study data sets display significantly *lower* rates of triadic closure than the null would predict. We then turn to degree assortativity in Section 5.2. Historically, degree assortativity has been computed on projected dyadic graphs and interpreted as a tendency toward interaction between productive or famous individuals. We show by example that the method of projection is in tension with this interpretation, and instead argue for the computation of assortativity coefficients directly on hypergraphs. We then study the effect of randomization on hypothesis tests for assortativity, showing that the choice between projected graph and hypergraph randomization is sufficient to drive conflicting study conclusions in both synthetic and empirical data sets. Finally, in Section 5.3, we consider the recently observed phenomenon of *simplicial closure* [26, 9]. We first illustrate the use of hypergraph configuration models to statistically test the hypothesis that triangles tend to close (be filled in by a 3-edge) at a higher-than-average rate, supporting this hypothesis in some but not all studied data sets. Direct measurements of simplicial closure on larger subgraphs can be both inflexible and combinatorially difficult to compute, so we suggest the *edge intersection profile* as an alternative measure. We illustrate the use of hypergraph models to compute null expectations for the intersection profile, and prove an asymptotic approximation which may be used for the analysis of data sets of arbitrary size. Both methods show our study data sets to have significantly larger intersections than the null expectation. We close in Section 6 with a summary of our findings and suggestions for future development.

2 Graphs, Simplicial Complexes, and Hypergraphs

Configuration models of dyadic networks have provided a flexible class of null models for many empirical studies over the last two decades. Configuration models are characterized by their preservation of the degree sequence of the original graph.

Definition 1 (Degree Sequence). *The degree sequence of a graph $G = (N, E)$ is a vector $\mathbf{d} \in \mathbb{R}^{|N|}$ whose u th entry is the number of edges incident on u :*

$$d_u = \sum_{v \in N} \mathbb{I}[(u, v) \in E] .$$

The configuration model is a probability distribution over the space of graphs that share a given degree sequence. This model was introduced by [16] as a probabilistic device through which to derive an asymptotic solution to a graph counting problem. The work of [17] studied the emergence of the giant component in these models. The authors of [21] gave alternative

derivations of these results, and subsequently provided some of the first examples of modeling real-world network data sets via configuration models. Subsequently, the configuration model was used to compute null expectations in the *modularity* function of a graph [27]. Modularity is an admittedly controversial ([28]) measure which is nevertheless central to contemporary community detection.

Recently, the authors of [25] distinguished two variants of the dyadic configuration model. The first is the *stub-labeled* configuration model, which coincides with the original model of [16, 17].

Definition 2 (Stub-Labeled Graphs). *For a fixed degree sequence \mathbf{d} , define the multiset*

$$\Sigma_{\mathbf{d}} = \bigsqcup_{v \in N} \{v_1, \dots, v_{d_v}\},$$

where \sqcup denotes multiset union. The copies v_1, \dots, v_{d_v} are stubs of node v . A stub-labeled graph is a partition $\{\{u_i, v_i\}\}_{i=1}^m$ of $\Sigma_{\mathbf{d}}$ into pairs such that $u_i \neq v_i$ for all i . We denote the space of stub-labeled graphs corresponding to degree sequence \mathbf{d} by $\mathcal{S}_{\mathbf{d},2}$.

The operation of partitioning $\Sigma_{\mathbf{d}}$ is often called “stub-matching”, and a stub-labeled graph is therefore an output of the stub-matching procedure. Importantly, a stub-labeled graph carries with it information about its construction. It is therefore distinct from our usual notion of a graph, which is instead captured by vertex labeling.

Definition 3 (Vertex-Labeled Graphs). *A vertex-labeled graph is a multiset of pairs of elements of N . We denote the space of vertex-labeled graphs with degree sequence \mathbf{d} by $\mathcal{V}_{\mathbf{d},2}$.*

There is a natural surjection $g : \mathcal{S}_{D,2} \rightarrow \mathcal{V}_{D,2}$. If $G \in \mathcal{S}_{D,2}$, $g(G) \in \mathcal{V}_{D,2}$ is the graph obtained by replacing each stub v_i in G with v and then consolidating the result as a multiset.

Definition 4 (Graph Configuration Models¹). *The vertex-labeled configuration model with degree sequence D is the uniform distribution $\eta_{\mathbf{d},2}^V$ on the space $\mathcal{V}_{\mathbf{d},2}$. Let $\lambda_{\mathbf{d},2}^S$ be the uniform distribution on $\mathcal{S}_{\mathbf{d},2}$. The stub-labeled configuration model with degree sequence D is the distribution $\eta_{\mathbf{d},2}^S = \lambda_{\mathbf{d},2}^S \circ g^{-1}$.*

The distinction between stub-labeled and vertex-labeled configuration models was elided in much previous applied literature due to the following two considerations. First, the stub-labeled and vertex-labeled models agree on the restricted space of *simple* graphs, which possess neither parallel edges nor self-loops. Second, in large, sparse graphs, the number of parallel edges and self-loops displays constant scaling, so the output of stub-matching will be “almost simple” and the distinction between labeling schemes negligible. However, as [25] points out, in many modern data sets we are not in the sparse regime, requiring the two models to be explicitly distinguished in order to obtain reliable data analytic results.

Considering the richness and importance of the dyadic configuration model, it is natural to seek generalizations to polyadic data. How is this to be done? A direct approach, taken in early studies such as [3], is to compute the *projected (dyadic) graph*. To construct the projected graph, for each observed k -adic interaction, draw an edge between each of the possible $\binom{k}{2}$ constituent pairs. This represents the interaction as a k -clique. The resulting graph may then be randomized according to vertex- or stub-labeled dyadic configuration models.

¹The configuration models defined here correspond to non-loopy multigraphs in the language of [25].

This approach, however, can have unintended and counterintuitive consequences. First, projecting determines what we are able to *measure*. All properties of interactions that depend on their dimension are immediately lost. Other observables such as node degrees and edge multiplicities can be transformed under projection in ways that can lead to unexpected results, as we show when we study degree-assortativity in Section 5.2. Second, even when our desired observable can be reliably measured on the projected graph, projection prior to randomization reflects an implicit choice of null space that may not be empirically motivated. For example, projecting an academic collaboration network prior to randomization implicitly chooses a null space in which almost all collaborations consist of exactly two authors; multiway collaborations arise “by coincidence” when the correct binary relationships are in place. This is a manifestly unrealistic model of academic collaboration, and a similarly unrealistic model of many other polyadic structures. Dyadic randomization of polyadic data may be appropriate in some circumstances, but the implicit choice to view dyadic relationships as “atomic” or “fundamental” in the null space is all-too-often left unquestioned.

Issues such as these motivate the development of explicitly polyadic data representations. These representations allow the analyst to choose both whether and when to project the data. In particular, they allow for randomization prior to any further data transformations, thereby enabling benchmarks against more relevant null spaces. We now make survey of efforts to define configuration-type models on such polyadic structures.

Random Simplicial Complexes

One recent family of polyadic configuration models defines a uniform distribution over a constrained subset of the space *simplicial complexes*. Simplicial complexes are fundamental objects in algebraic topology and topological data analysis, with many convenient properties. Simplicial complexes may be viewed as a subspecies of hypergraphs, which we therefore define first.

Definition 5 (Hypergraph). *A (vertex-labeled) hypergraph $G = (N, E)$ consists of a node set N and an edge set $E = \{\Delta_j\}_{j=1}^m$ which is a multiset of subsets of N . Each subset is called a hyperedge or simplex. We denote by \mathcal{V} the space of vertex-labeled hypergraphs.*

Remark. In this definition, we have excluded generalized self-loops (edges in which a single node i appears multiple times), but allowed parallel edges (distinct indices $i \neq j$ such that $\Delta_i = \Delta_j$.)

Definition 6 (Simplicial Complex). *Hypergraph G is a simplicial complex if, for all $\Delta \in G$ and each $\Gamma \subset \Delta$, it holds that $\Gamma \in G$.*

The subset Γ is often called a *facet* of Δ . If Δ is not a proper facet of any other simplex, Δ is also called a *face* of the complex. It follows that a simplicial complex can be completely described by its set of faces, since the presence of all their facets is then implied. This feature makes simplicial complexes especially attractive tools for studying topological features in data [29], since they can be compactly represented by a subset of the data while preserving macroscopic topological structure.

Perhaps for these reasons, simplicial complexes have occupied much of the recent attention from the network science community. Indeed, a recent paper [23] refers to simplicial complexes as “the high-order generalization of a network,” implying that the choice of generalization is unique. There are now at least two models [23, 24] laying claim to the title

of “simplicial configuration model.” The model of [24] achieves analytic tractability by restricting to simplicial complexes with faces of uniform dimension, while the model of [23] allows heterogeneous dimensions but sacrifices analytic tractability. In addition to these configuration-type models, there is an increasing number of physically and geometrically-inspired random simplicial complex processes [30, 31, 32, 33, 34, 35].

Simplicial complexes are compact constructions with elegant properties. As with projected graphs, however, the choice to transform the data prior to measurement or randomization has downstream consequences on study conclusions that must be reckoned with. By design, a representation of a data set as a simplicial complex discards information about the occurrence of faces of maximal simplices. This simplification is a feature when it is desirable to parsimoniously represent topological properties of the data in question, since such features are usually defined via reference only to facets. When the design principles of the studied network are explicitly structural – as may occur in brain networks [36] and protein-protein interaction networks [37] – such features may be the fundamental objects of interest. Generically, however, simplicial complex representations inhibit reliable measurements of *local* properties such as node degrees, clustering, and assortativity. This in turn has consequences for downstream analyses that depend on these properties, such as community detection. Worse, recent work [9] has found that such local properties interact strongly with traditionally topological ones, indicating that it is easier to predict the topological evolution of a data set when local properties are explicitly represented.

Transforming the data via simplicial simplification also incorporates strong assumptions into the corresponding null models. Figure 1 shows two toy collaboration networks G_1 and G_2 and their representations as simplicial complexes. Each network contains four collaborations, two between three nodes and two between two. The two networks differ only by a parallel edge swap $(A, B), (C, D) \mapsto (A, D), (B, C)$. As a result, G_1 and G_2 have identical degree sequences and edge dimension sequences. Indeed, they share a somewhat stronger property: each node participates in the same number of collaborations of each dimension. In both G_1 and G_2 , node A has one collaboration of size 3 and one of size 2; node B two of size 3 and one of size 2, and so on. However, these similar collaboration hypergraphs G_1 and G_2 have distinct representations as simplicial complexes S_1 and S_2 , since edge (A, D) constitutes a maximal clique in the bottom graph. Because of this, the configuration space defined by S_1 does not include S_2 , and therefore implicitly excludes G_2 as well.

A uniform null model defines a space of equally-weighted, counterfactual realizations of the observed data. While a configuration model is meant to define a non-informative distribution over such a space, the simplicial configuration model defined by S_1 is strongly opinionated about the possible locations of pairwise collaborations in the original data. It is direct to verify that S_1 is in fact the only element of its null space, and therefore only pairwise collaborations consistent with S_1 are included. Since (A, D) is not a facet of S_1 , the use of the configuration model in this context deterministically excludes any occurrences of (A, D) from the null space. This simple example illustrates a more general phenomenon: simplicial configuration models implicitly condition on the occurrence of a specific set of maximal simplices, and thereby assume all edges in the original hypergraph to be sub-faces of the observed maximal simplices. In practice, this may be a very strong modeling assumption. On the other hand S_1 and S_2 are each consistent with arbitrary numbers of repetitions of their given edges. A configuration model on S_1 thus views a counterfactual data set in which edge (A, B) is repeated 1,000 times as a relevant comparison to the observed data – but insists that S_2 is not. While this behavior may be desirable in a given context, it is necessary to explicitly account for it in the interpretation of analyses driven by simplicial

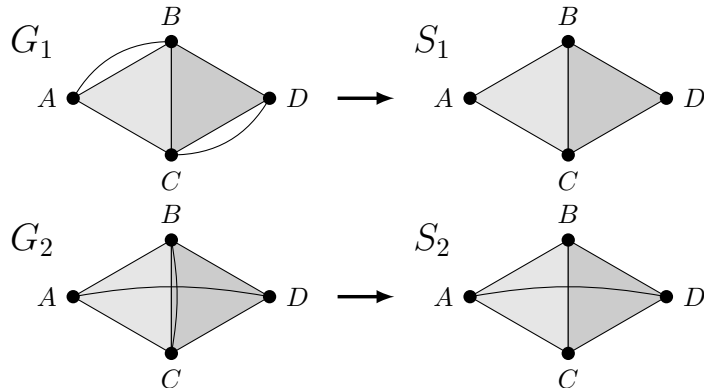


Figure 1: (Left): Two collaboration networks with the same node degree and edge dimension sequences. Filled triangles represent three-way collaborations. (Right): The two networks have different representations as simplicial complexes, since collaboration $A - D$ is maximal the bottom network.

null models.

Random Hypergraphs

Hypergraphs are a natural representation of polyadic interaction data sets – each interaction is explicitly represented by a hyperedge over its node set. It is therefore natural to define null models directly on the space of hypergraphs. Extant literature provides several approaches. One takes a somewhat indirect route through *bipartite graphs*. A bipartite graph is a graph containing two types of nodes, in which connections are allowed only between nodes of differing types. There is a simple bijection between stub-labeled hypergraphs and bipartite graphs. To construct a bipartite graph B from a hypergraph G , we create one layer of nodes in B corresponding to the nodes N of G , and a second layer in B corresponding to the edges E of G . A node v is linked to an edge-node e iff $v \in e$ in the original hypergraph G . G may be recovered by “projecting” B onto the node layer. The authors of [21] were the first to define a (network) configuration model on the space of bipartite graphs. As they show, the process of randomizing over bipartite graphs, projecting onto the node layer to obtain a hypergraph, and then projecting that hypergraph onto its dyadic line graph can yield realistic results. The authors of [22] develop an alternative null model on the space of bipartite graphs, which they refer to as a “configuration model” despite being more closely related to the model of Chung and Lu [38].

Some studies have also defined distributions directly over spaces of hypergraphs. In [18], the authors define an analog of the stub-labeled configuration model over 3-uniform hypergraphs (in which all edges have three nodes) in the service of studying a tripartite tagging network on an online platform. A few more general models have been developed for the purposes of community-detection in hypergraphs via modularity maximization. Any definition of modularity requires a method for computing a null probability for the presence of an edge on any given tuple of nodes. In [19], the authors develop a degree-preserving randomization via a “corrected adjacency matrix,” which may then be used for modularity maximization on the projected graph. In [20], the authors explicitly generalize the Chung-Lu

model to non-uniform hypergraphs with arbitrary expected degree sequences in the service of defining the modularity function.

These hypergraph null models are all of independent interest. None of them, however, directly address the problem of hypothesis-testing on polyadic data sets. For example, the bipartite randomization of [21] generalizes the stub-labeled configuration model of [25], and is therefore equivalent to the stub-labeled hypergraph model we define in Section 4. However, many polyadic data sets are most appropriately studied in vertex-labeled spaces and there is no natural analog to a vertex-labeled configuration model on bipartite graphs. The Chung-Lu model and its variants have similar degree expectations but dramatically different probabilistic structure, making it unsuitable for hypothesis-testing. These considerations motivate the development of flexible configuration models directly on hypergraph spaces.

3 Configuration Models of Random Hypergraphs

Throughout our development, calligraphic characters such as \mathcal{R} , \mathcal{V} , and \mathcal{S} refer to spaces of hypergraphs. Individual hypergraphs are written $G = (N, E)$, where G is the graph object, N the node set, and E the edge-set. The exact nature of the edge-set depends on the space in which G lives, and is discussed below. A single, random edge in E is given by capital and lowercase Greek characters, e.g. $\Delta = (\delta_1, \dots, \delta_\ell)$. A fixed tuple of vertices of N is given by capital and lowercase English characters, e.g. $R = (r_1, \dots, r_\ell)$. A statement such as $\Delta = R$ describes the event that the random edge Δ has fixed location R .

Model Definitions

The space \mathcal{V} of vertex-labeled hypergraphs was defined in Definition 5. As argued in [25], \mathcal{V} is the natural space for a wide range of network data sets. Our general aim is to define an appropriately ignorant null distribution over \mathcal{V} and \mathcal{S} , the space of stub-labeled hypergraphs.

Definition 7. Fix \mathbf{d} and let

$$\Sigma = \bigsqcup_{v \in N} \{v_1, \dots, v_{d_v}\} ,$$

A stub-labeled hypergraph is a partition of Σ such that no two stubs of the same node v are contained in the same equivalence class. We denote the space of stub-labeled hypergraphs by \mathcal{S} .

Remark. There is a natural surjection $g_{\mathcal{S}} : \mathcal{S} \rightarrow \mathcal{V}$. If $G \in \mathcal{S}$, $g_{\mathcal{S}}(G) \in \mathcal{V}$ is the hypergraph obtained by replacing each stub v_i in G with v and then consolidating the result as a multiset.

Having defined the spaces upon which our models live, we may now define the constraints that give those models structure.

Definition 8 (Incidence Matrix). The incidence matrix $I(G)$ of a hypergraph G is an $n \times m$ matrix defined entrywise as

$$I(G)_{ij} = \begin{cases} 1 & v_i \in e_j \\ 0 & \text{otherwise} . \end{cases}$$

Let $n = |N|$ and $m = |E|$. Denote by \mathbf{e} the vector of ones; its dimension will be clear in context.

Definition 9 (Degree and Dimension Sequences). *The degree sequence of G is the vector of row sums $\mathbf{d} = I(G)\mathbf{e}$, where \mathbf{e} denotes the appropriately-sized constant vector of 1s. The i th entry d_i of \mathbf{d} gives the number of edges incident to node v_i . The dimension sequence of G is the vector of column sums $\mathbf{k} = \mathbf{e}^T I(G)$. The j th entry k_j of \mathbf{k} gives the number of nodes in edge e_j . We denote by deg and dim the functions that assign to a given hypergraph G its degree and dimension sequences.*

Definition 10 (Configuration Models). *The vertex-labeled configuration model with degree sequence \mathbf{d} and edge dimension sequence \mathbf{k} is the uniform distribution on the set*

$$\mathcal{V}_{\mathbf{d},\mathbf{k}} = \{G \in \mathcal{V} \mid \text{deg}(G) = \mathbf{d}, \text{dim}(G) = \mathbf{k}\} .$$

Let $\lambda_{\mathbf{d},\mathbf{k}}$ be the uniform distribution on the set

$$\mathcal{S}_{\mathbf{d},\mathbf{k}} = \{G \in \mathcal{S} \mid \text{deg}(G) = \mathbf{d}, \text{dim}(G) = \mathbf{k}\} .$$

The corresponding stub-labeled configuration model is $\eta_{\mathbf{d},\mathbf{k}}^{\mathcal{S}} = \lambda_{\mathbf{d},\mathbf{k}} \circ g^{-1}$, the distribution induced by $\}$.

Remark. For notational compactness, we may repress the space, \mathbf{d} , or \mathbf{k} when these are clear in context.

Modeling Considerations

In practice, the analyst utilizing a configuration null model must choose a space in which to work. In [25], the authors consider three data-scientific case studies, and address the question of whether stub- or vertex-labeling is most appropriate for defining a null model. In each case, their choice is guided by the logic of the underlying interaction structure. Roughly, in cases when permutations of stubs generate distinct, valid structures, the authors argue that the appropriate space is stub-labeled. In contrast, when stub-permutations are either nonsensical or leave the interaction structure unchanged, vertex-labeling is to be preferred. For example, in the collaboration network of computational geometers, the authors implicitly identify stubs with “participations” in a collaboration. Since author A’s first participation in a collaboration with author B cannot logically be B’s first participation in a collaboration with A, permutations of the stubs do not generate valid interaction structures and stub-labeling is therefore ruled out. The authors therefore analyze this network via vertex-labeled configuration models. Many other data sets that arise as interactions between distinguishable agents are appropriately studied via vertex-labeling for similar reasons.

4 Sampling Random Hypergraphs

We now consider the problem of sampling from the models defined in Section 3. To do so, we develop a Metropolis-Hastings algorithm for approximate sampling from stub- and vertex-labeled configuration models. This algorithm uses a simple step – the pairwise edge reshuffle – to systematically explore the relevant hypergraph spaces. Tuning the acceptance probabilities allows the algorithm to sample from either $\mathcal{S}_{\mathbf{d},\mathbf{k}}$ or $\mathcal{V}_{\mathbf{d},\mathbf{k}}$.

Metropolis-Hastings is a particularly useful form of Markov Chain Monte Carlo (MCMC), which employs a Markov chain whose states are elements of the set to be sampled. Fix \mathbf{d} and \mathbf{k} . Let $\mathcal{R} \in \{\mathcal{S}_{\mathbf{d},\mathbf{k}}, \mathcal{V}_{\mathbf{d},\mathbf{k}}\}$ be the desired null space of hypergraphs. A chain on \mathcal{R} which is (a) ergodic and (b) reversible under $\eta^{\mathcal{R}}$ has $\eta^{\mathcal{R}}$ as its equilibrium measure. States sampled at sufficiently-long intervals from this chain are then approximately i.i.d. according to $\eta^{\mathcal{R}}$. The Metropolis-Hastings method provides a recipe for constructing such a chain. We require a *proposal distribution* describing how to move from one state to another. To develop the proposal distribution, it is convenient to work first on the stub-labeled space \mathcal{S} .

Definition 11 (Pairwise Reshuffle). *Let $G \in \mathcal{S}$. Let $\Delta, \Gamma \in G$. A pairwise reshuffle $b(\Delta, \Gamma|G)$ of Δ and Γ is a sample from the conditional distribution $\eta(\cdot|E \setminus \{\Delta, \Gamma\})$.*

Since all hyperedges other than Δ and Γ are fixed in a pairwise reshuffle, we may view $b(\Delta, \Gamma)$ either as a random map on stub-labeled hypergraphs $G \mapsto G'$ or as a random map on pairs of hyperedges $(\Delta, \Gamma) \mapsto (\Delta', \Gamma')$. When no possibility of confusion arises, we will therefore abuse notation and write either $b(\Delta, \Gamma|G) = G'$ or $b(\Delta, \Gamma|G) = (\Delta', \Gamma')$ as appropriate.

Lemma 1 (Pairwise Reshuffle Algorithm). *A pairwise reshuffle of hyperedges $\Delta, \Gamma \in G$ may be carried out as follows.*

1. Delete Δ and Γ from E .
2. Construct Δ' and Γ' as (initially empty) node sets.
3. For each node $v \in \Delta \cap \Gamma$, add a v -stub to both Δ' and Γ' .
4. From the set $\Delta \Delta \Gamma$, select $|\Delta \setminus \Gamma|$ stubs u.a.r. and add them to Δ' . Add the remainder to Γ' .
5. Add Δ' and Γ' to E .

Proof. It suffices to note that the pairwise reshuffle measure is conditioned from a uniform measure, and is therefore again uniform. The algorithm above generates a uniform sample from the set of possible configurations of Δ and Γ conditioned on the remainder of the hypergraph, as required. \square

The clauses of Corollary 1 follow immediately from Lemma 1.

Corollary 1. *Let $G \in \mathcal{S}$. Let $b(\Delta, \Gamma|G) = \Delta', \Gamma'$ be a pairwise reshuffle which results in new graph $G' \in \mathcal{S}$. Then,*

1. *The degree and dimension sequences are preserved: $\deg(G) = \deg(G')$ and $\dim(G) = \dim(G')$.*
2. *Local intersections and unions are preserved: $|\Delta| = |\Delta'|$, $|\Gamma| = |\Gamma'|$, and $|\Delta \cap \Gamma| = |\Delta' \cap \Gamma'|$.*

Corollary 2. *Let $b(\Delta, \Gamma|G)$ be a pairwise reshuffle. Any valid reshuffle occurs with probability*

$$q_{\mathcal{S}}(\Delta, \Gamma) = 2^{-|\Delta \cap \Gamma|} \binom{|\Delta| + |\Gamma| - 2|\Delta \cap \Gamma|}{|\Delta| - |\Delta \cap \Gamma|}^{-1}.$$

Proof. There are $2^{|\Delta \cap \Gamma|}$ ways to assign duplicate stubs in the intersection $\Delta \cap \Gamma$. There are $\binom{|\Delta|+|\Gamma|-2|\Delta \cap \Gamma|}{|\Delta|-|\Delta \cap \Gamma|}$ ways to partition these stubs between $\Delta \setminus \Gamma$ and $\Gamma \setminus \Delta$. \square

We now define a proposal kernel on the space \mathcal{S} . Write $G \sim_{\Delta, \Gamma} G'$ if there exists a pairwise shuffle b such that $b(\Delta, \Gamma | G) = G'$. If such a pair Δ and Γ do exist, they are unique (recall that we are working in the space of stub-labeled hypergraphs). Then, let

$$p_{\mathcal{S}}(G' | G) = \begin{cases} \binom{m}{2}^{-1} q(\Delta, \Gamma) & G \sim_{\Delta, \Gamma} G' \\ 0 & \text{otherwise.} \end{cases}$$

To sample from $p_{\mathcal{S}}(\cdot | G)$, it suffices to sample two uniformly random edges from G and then pairwise reshuffle them according to Lemma 1. The prefactor $\binom{m}{2}^{-1}$ gives the probability that any two given edges are chosen.

Theorem 1. *The Markov chain on \mathcal{S} defined by the kernel $p_{\mathcal{S}}$ is aperiodic, irreducible, and reversible with respect to $\eta^{\mathcal{S}}$.*

Proof. Our proof approach generalizes that of [25]. We first show aperiodicity by showing that $p_{\mathcal{S}}$ contains both a cycle of length 2 and a cycle of length 3. If $m = 1$, $p_{\mathcal{S}}$ is trivially aperiodic since the space contains a single configuration. If $m > 1$, we may construct a cycle of length 2 by performing the reshuffles $\Delta, \Gamma \mapsto \Delta', \Gamma'$ followed by $\Delta', \Gamma' \mapsto \Delta, \Gamma$ for any distinct edges Δ and Γ . To construct a cycle of length 3, let $\Delta = (\delta_1, \delta_2, \dots, \delta_k)$ and $\Gamma = (\gamma_1, \gamma_2, \dots, \gamma_\ell)$ for $k, \ell \geq 2$. Then, execute the reshuffles

$$\begin{aligned} (\delta_1, \delta_2, \dots, \delta_k), (\gamma_1, \gamma_2, \dots, \gamma_\ell) &\mapsto (\gamma_1, \delta_2, \dots, \delta_k), (\delta_1, \gamma_2, \dots, \gamma_\ell) \\ &\mapsto (\gamma_1, \gamma_2, \dots, \delta_k), (\delta_1, \delta_2, \dots, \gamma_\ell) \\ &\mapsto (\delta_1, \delta_2, \dots, \delta_k), (\gamma_1, \gamma_2, \dots, \gamma_\ell), \end{aligned}$$

arriving at the initial configuration after three transitions. Since 2 and 3 are relatively prime, $p_{\mathcal{S}}$ is aperiodic, as was to be shown.

To show reversibility with respect to $\eta^{\mathcal{S}}$, we compute, for any $G \sim_{\Delta, \Gamma} G'$,

$$p_{\mathcal{S}}(G' | G) = \binom{m}{2}^{-1} q(\Delta, \Gamma) = \binom{m}{2}^{-1} q(\Delta', \Gamma') = p_{\mathcal{S}}(G | G'). \quad (1)$$

The second equality follows from Corollary 1, since $q(\Delta, \Gamma)$ depends only on $|\Delta|$, $|\Gamma|$, and $|\Delta \cap \Gamma|$.

We will now demonstrate irreducibility by constructing a path of nonzero probability between any distinct G_1 and G_2 in \mathcal{S} . Let E_1 and E_2 be the edge-sets of G_1 and G_2 , respectively. We first describe a procedure for generating a new graph G_3 such that $|E_2 \setminus E_3| < |E_2 \setminus E_1|$. The path is then constructed by applying this procedure inductively.

Since $E_1 \neq E_2$ and $|E_1| = |E_2|$, we may pick $\Delta = (r_1, \dots, r_\ell) \in E_2 \setminus E_1$. Note that each r_i in Δ is a stub. Note further that, since $\Delta \notin E_1$, there exists an edge $\Psi \in E_1 \setminus E_2$ such that $|\Psi| = \ell$. Now, for each i , since $\Delta \notin E_1$, r_i belongs to a different edge (call it Γ_i) in E_1 . Since r_i is a stub, r_i can belong to only one edge in each graph, and therefore $\Gamma_i \notin E_2$. In general, we may have $j \neq \ell$ since we may have $\Gamma_i = \Gamma'_i$ when two stubs belong to the same edge in E_1 . Relabel stubs if necessary to obtain distinct hyperedges $\Gamma_1, \dots, \Gamma_j$. We first perform the shuffle $\Psi^{(0)}, \Gamma_1^{(0)} = b^{(0)}(\Psi, \Gamma_1)$ such that $\Delta \cap (\Gamma_1 \cup \Psi) \in \Psi^{(0)}$. To construct such a shuffle, simply assign all stubs $r_i \in \Delta$ to $\Psi^{(0)}$, and then uniformly distribute any remaining

stubs. We now construct a sequence of pairwise reshuffles by which $Psi^{(0)}$ is transformed into Δ . For each $i = 2, \dots, j$, let $\Psi^{(i)}, \Gamma_i^{(1)} = b^{(i)}(\Psi^{(i-1)}, \Gamma_i)$, where $b^{(i)}$ assigns all elements of Δ in $\Psi^{(i-1)} \cup \Gamma_i$ to $\Psi_i^{(i)}$ and uniformly distributes the rest. Since $\Delta \in \Psi^{(0)} \cap \bigcap_{i=2}^j \Gamma_i$ by construction, by the end of this procedure we have $\Psi^{(j)} = \Delta$. Call the resulting graph G_3 with edge set E_3 . Since we have only modified the edges $\{\Gamma_i\}$ and Ψ , which are elements of $E_1 \setminus E_2$, we have not added any edges to the set $E_1 \setminus E_2$, but we have removed one (Ψ). We therefore have $|E_2 \setminus E_3| \leq |E_2 \setminus E_1| = 1$, as was to be shown. \square

Corrolary 3. *The Markov chain on \mathcal{S} generated by $p_{\mathcal{S}}$ has $\eta^{\mathcal{S}}$ as its unique equilibrium distribution.*

We now turn attention to sampling from the vertex-labeled model $\eta^{\mathcal{V}}$. We first modify the proposal kernel. In vertex-labeled spaces, any given pairwise reshuffle occurs with probability $q_{\mathcal{V}}(\Delta, \Gamma) = \left(\frac{|\Delta| + |\Gamma| - 2|\Delta \cap \Gamma|}{|\Delta| - |\Delta \cap \Gamma|} \right)^{-1}$; the dropped first factor reflects the fact that there is only one valid assignment for the intersection under vertex labeling. Additionally, we must account for the fact that parallel edges are equivalent in vertex-labeled spaces, and requiring down-sampling of transitions. Define the *acceptance probability*

$$a_{\mathcal{V}}(G'|G) = a_{\mathcal{V}}(\Delta', \Gamma' | \Delta, \Gamma) = \begin{cases} 0 & \Delta = \Delta' \text{ or } \Delta = \Gamma' \\ \frac{1}{m_{\Delta} m_{\Gamma}} & \text{otherwise,} \end{cases}$$

where m_{Δ} is the multiplicity of edge Δ in G . This factor reflects the fact that, for any swap of Δ and Γ , there are $m_{\Delta} m_{\Gamma}$ choices of initial edges to sample parallel to Δ and Γ , all of which generate the same element of \mathcal{V} . For notational convenience, we also define $a_{\mathcal{S}}(G, G') = 1$.

Corrolary 4. *Let*

$$p_{\mathcal{V}}(G'|G) = \begin{cases} \binom{m}{2}^{-1} q_{\mathcal{V}}(\Delta, \Gamma) a(G'|G) & G' \sim_{\Delta, \Gamma} G \\ 0 & \text{otherwise.} \end{cases}$$

The kernel $p_{\mathcal{V}}$ is aperiodic, irreducible, and reversible with respect to $\eta^{\mathcal{V}}$.

Proof. Reversibility can be verified by direct computation along the lines of Equation (1). Aperiodicity and irreducibility directly follow from the aperiodicity and irreducibility of $p_{\mathcal{S}}$. \square

Having defined the required Markov chains, we formalize our procedure in Algorithm 1.

Algorithm 1 Metropolis-Hastings for Hypergraph Configuration Models

Data: \mathbf{d}, \mathbf{k} , space $\mathcal{R} \in \{\mathcal{S}_{\mathbf{d},\mathbf{k}}, \mathcal{V}_{\mathbf{d},\mathbf{k}}\}$, sample interval $M \in \mathbb{Z}_+$

Result: j hypergraphs

initialization: $i \leftarrow 1, G \leftarrow G_0 \in \mathcal{R}$

while $i \leq jM$ **do**

 sample (Δ, Γ) u.a.r. from G

$G' \leftarrow b(\Delta, \Gamma | G_{i-1})$

 Let $U \sim \text{unif}(0, 1)$. **if** $U < a_{\mathcal{R}}(G, G')$ **then**

 | $G_i \leftarrow G'$ $i \leftarrow i + 1$

else

 | **pass**

end

end

return $\{G_i \text{ such that } i|M\}$

Since the given chains are ergodic and reversible, we immediately obtain the following guarantee:

Theorem 2. *A set of j samples produced by Algorithm 1 converges in distribution to the desired product measure $\eta^{\otimes j}$ as $M \rightarrow \infty$.*

Informally, if the sampling interval is large enough, a sequence of graphs G_1, \dots, G_j will be arbitrarily close to being independent and identically-distributed from η . We are, however, unaware of any results giving approximate scaling of M for this class of Markov chains. As a result, it is possible in principle that the scaling in M as a function of graph size is extremely poor. Experience indicates, however, that samples can be extracted from networks with hundreds of thousands of edges on personal computing equipment in practical time.

5 Three Applications

We now demonstrate the utility of hypergraph configuration models via applications to three simple network analyses. In Section 5.1, we consider a classical measure – the average clustering coefficient of a network. The study of clustering in [39] and related works was one of the earliest results in modern network science. It is often said that social and collaboration networks display “nonrandom” or “significant” levels of clustering. We will see, however, that many polyadic networks in fact display *less* clustering than would be expected under randomization via hypergraph configuration models, and discuss some of the physical interpretations of this finding.

We turn to degree-assortativity in Section 5.2. We first show that computing dyadic assortativity on projected graphs can lead to results at odds with our intuition about collaboration and social networks. We define three notions of assortativity on hypergraphs, each of which measure different kinds of association. We then compare observed degree assortativity in a range of study data-sets to hypergraph and projected graph null models, finding that the use of hypergraphs can both change the sign of observed assortativity coefficients and determine the statistical significance of study conclusions.

Finally, in Section 5.3, we define a new, intrinsically polyadic metric for hypergraphs – the intersection distribution – and relate it to the phenomenon of simplicial closure. Unlike

clustering and assortativity, which are natively dyadic measures, the intersection distribution can only meaningfully be computed in hypergraphs. The intersection distribution requires contextualization via null models; we find using computational and analytic methods that a variety of data sets display higher rates of edge-intersections than would be expected by chance. These three case studies underscore the importance of correctly-specified null models in studying empirical data sets, and speak toward the use of hypergraph null models in data scientific practice.

The data sets for each application section were gathered, cleaned, and generously made public by the authors of [9]. In certain experiments, data were temporally subsetted in order to reduce size; these cases have been explicitly noted in the text and the subsetting described in Appendix B. Importantly, in no case was the subsetting motivated by the runtime of Algorithm 1; rather, the bottlenecks were standard, expensive computations such as triangle counting.

5.1 Trivializing Triadic Closure

The study of “clustering” in networks has occupied attention since the advent of modern network science, coming to fore with the publication of the seminal paper of Watts and Strogatz [39]. The intuition of clustering is simple: in many networks, if two u and v interact with a third node w , then there is an elevated propensity for u and v to interact with each other. This phenomenon is often called *triadic closure*. The prototypical example is in social networks, where clustering reflects the tendency of people who share acquaintances to be acquainted as well. Traditionally, clustering in networks is measured by a ratio of the number of triangles (closed cycles on three nodes) are present in the graph, compared to the number of “wedges” (subgraphs on three nodes in which two edges are present).² Local and global variations of this ratio may be formulated. Rather than deeply investigating the relative merits of these measures, we will simply follow the choice of [39] and work with the *average local clustering coefficient*. The local clustering coefficient at node v is defined as follows. We first count the number of triangles T_v incident on v . The number of wedges W_v incident on v is number of distinct pairs of nodes connected to v , and is therefore $W_v = \binom{d_v}{2}$. The local clustering coefficient at v is then

$$C_v = \frac{T_v}{W_v}.$$

In turn, the average local clustering coefficient is

$$\bar{C} = \frac{1}{|N|} \sum_{v \in N} C_v.$$

Many empirical networks display nonzero clustering coefficients. While some of these networks—such as online friendship networks—are natively dyadic, others—such as collaboration networks—are natively polyadic. The distinction has often been elided in analyses which proceed by first computing the dyadic graph. Comparison to the dyadic configuration model then yields a significant finding of triadic closure, since it is well known that \bar{C} converges to zero in the sparse configuration model as n grows large (see e.g. [41]). Largely through such dyadic studies, it has become common wisdom that empirical networks display more triadic closure than would be expected by random chance.

²Though recent measures have been developed for higher-order notions of clustering on larger subgraphs as well; see [40].

	\bar{C}	Hypergraph		Projected	
		Vertex	Stub	Vertex	Stub
coauth-MAG-Geology*	0.82	0.81 (0.00)	0.81 (0.00)	0.00 (0.00)	0.00 (0.00)
NDC-classes*	0.60	0.58 (0.02)	0.60 (0.02)	0.01 (0.00)	0.01 (0.00)
email-Enron	<i>0.66</i>	0.84 (0.01)	0.81 (0.01)	0.03 (0.00)	0.04 (0.01)
email-Eu*	<i>0.54</i>	0.62 (0.01)	0.64 (0.01)	0.00 (0.00)	0.00 (0.00)
congress-bills*	<i>0.61</i>	0.83 (0.00)	0.81 (0.00)	0.00 (0.00)	0.05 (0.00)
tags-ask-ubuntu*	<i>0.57</i>	0.61 (0.01)	0.63 (0.01)	0.00 (0.00)	0.03 (0.01)
threads-math-sx*	<i>0.29</i>	0.40 (0.01)	0.42 (0.01)	0.00 (0.00)	0.00 (0.00)

Table 1: Average local clustering coefficients for selected data sets, compared to the distributions computed under vertex- and stub-labeling of hypergraph and projected graph models. Parentheses show two standard deviations under the equilibrium distribution of each model. **Bold** observed values of \bar{C} are at least two standard deviations greater than its expectation under either hypergraph null, while *italic* values are at least two standard deviations lower. Starred* data sets have been temporally subsetted as described in Appendix B.

Triadic closure, however, can have both trivial and nontrivial sources. As [4] points out, there is a trivial driver (groups of three or more generate closed triangles when edges are projected onto cliques), as well as a possible nontrivial driver (the tendency of distinct groups to overlap). To evaluate whether natively polyadic networks display *nontrivial* clustering requires averaging out the impact of the trivial driver. This is precisely a task for a polyadic null model.

We performed a sequence of experiments shown in Table 1. For each polyadic data set, we constructed the empirical unweighted projected graph, and subsequently the average local clustering coefficient \bar{C} . We then compared the observed value to its distribution under four randomizations. We first randomized using the vertex- and stub-labeled hypergraph configuration models, *prior* to projecting down to the line graph and measuring \bar{C} (second and third columns). We then reversed the order of projection and randomization in the fourth and fifth columns, first computing the projected graph and then applying the dyadic configuration models.

The empirical values of \bar{C} range from 0.29-0.82, reflecting large amounts of triadic closure in the projected graph. These values, however, require benchmarks for interpretation. Benchmarking against either of the dyadic configuration models gives predictable results – regardless of labeling, all data sets would be found to display extremely “significant” clustering. However, the dyadic nulls fail to separate trivial from nontrivial clustering drivers. Randomizing via the hypergraph null models yields strikingly different conclusions using either the vertex-labeled or stub-labeled spaces. Of the data sets shown, only **coauth-MAG-Geology** and **NDC-classes** show a higher degree of clustering than expected under hypergraph configuration models, and then by very small margins. Of the two, only the former is statistically significant. In contrast, the other data sets display much *less* triadic closure than would be expected by random chance. Not only is there no nontrivial clustering; triadic closure seems to even be discouraged in many of these data sets.

Why would these networks display less triadic closure than would be expected by chance?

The answer to this question is presumably depends on the domain of each data set. In the context of the two email networks, there may be an intuitive explanation for this phenomenon. On short timescales, cycles of distinct emails may correspond to redundant communication, in which information is transmitted to agents who already possess it. Because of this, such networks may tend to display fewer short cycles, and therefore smaller values of \bar{C} . The lower-than-expected clustering coefficient in the Congressional cosponsorship data may reflect a tendency for bill content to be strategically consolidated into large packages – counterfactual bills that could otherwise form a cycle in the graph may instead be grouped into existing bills. If true, both of these phenomena would illustrate a tendency for potential cycles to be “absorbed” into higher-dimensional edges, hinting toward the importance of studying high-dimensional edges directly as we do in Section 5.3.

It is possible to make different methodological choices in the performance of these experiments. One important choice relates to the use of the unweighted projected graph. It would be possible to weight the edges in the projected graph using information from the hypergraph, and then apply a weighted clustering coefficient. We have specifically chosen the unweighted projection when computing coefficients because this matches historical practice in studying triadic closure on polyadic data. As we have shown, this approach plays an oft-unremarked role in determining study findings. First transforming and then randomizing would conclude that all studied data sets display triadic closure. In contrast, randomizing first allows us to separate trivial and nontrivial clustering effects. Doing so suggests that many polyadic data sets – including some social and collaboration networks – display a significant tendency *away* from triadic closure. The choice of null models has the power to substantially alter our views of even familiar network measures.

5.2 Degree Assortativity: Measurement and Generalizations

A network is *assortative* when “similar” nodes tend to be connected to each other at higher rates than “dissimilar” nodes. In general terms, assortativity is to be expected when networks are formed by processes in which similar nodes preferentially interact with each other. For example, many social networks are assortative by age, race, political affiliation, and socioeconomic status [42]. In contrast, *disassortativity* is to be expected when interactions require or are encouraged by the presence of nodes with differing identities or roles. A radical example would be a heterosexual dating network, which is by definition disassortative by gender.

An especially important form of assortativity is *degree*-assortativity, in which the attribute assigned to each node is simply the number of its neighbors. Degree-assortativity has been found to distinguish structural categories of empirical networks. Some of the earliest studies on degree-assortativity [43, 44, 45] found that a variety of social, biological, and infrastructural networks display different kinds of degree-assortative mixing. In social networks, these observations have often been taken as evidence of a tendency of successful and productive agents to work together.

Degree-assortativity in binary networks is often measured via a correlation coefficient. Let $g : N \rightarrow \mathbb{R}$ be a function that assigns to each node a scalar attribute. The general assortativity correlation coefficient is

$$\rho_{\text{proj}} = \frac{\langle g(u)g(v) \rangle - \langle g(u) \rangle^2}{\langle g(u)^2 \rangle - \langle g(u) \rangle^2},$$

where $\langle \cdot \rangle$ denotes the empirical average in which each edge is sampled once, with u and v

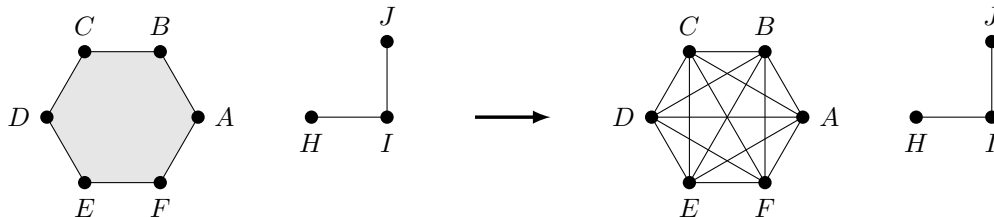


Figure 2: A toy coauthorship network with $n = 9$ nodes. On the left, the network represented as a hypergraph with 3 hyperedges. On the right, the projected graph with 17 dyadic edges.

the nodes at either end of the edge. When $g(u) = d_u - 1$, the remaining degree of u , ρ_g is the Pearson correlation coefficient of node degrees used by [44] and many subsequent studies. Pearson coefficients suffer from pathological behavior in the limit of large, sparse graphs ([46]), and so we instead use the Spearman rank correlation coefficient. The Spearman coefficient is obtained by setting $g(u)$ equal to the rank of the degree of node u in the set of samples. We use Spearman coefficients in all subsequent analysis, although on our data sets the difference between the Spearman and Pearson coefficients is negligible.

How should assortativity be studied in hypergraphs? The historical approach has been to construct the projected graph, after which correlation coefficients may be computed as usual. This approach, however, can raise difficulties. Observed assortativity is often attributed to the tendency of extremely productive scholars to collaborate with each other. However, the projection operation significantly complicates the interpretability of these coefficients. Consider the toy coauthorship network shown in Figure 2. This network contains one collaboration with six authors and two collaborations of two authors each. The corresponding projected graph contains a 6-clique and two 2-cliques. Each node $A - F$ has degree $6 - 1 = 5$. Nodes G and I each have degree 1, while node H has degree 2. To compute the Spearman coefficient, we sample each of the 17 edges total edges in the graph twice (once in each orientation), computing for each the remaining degree of each node. We then rank the remaining degrees, and compute the correlation coefficient of the ranks. The Spearman rank correlation coefficient for degree assortativity in this case is 0.99, suggesting very strong degree assortativity.

Clearly, the strong degree assortativity in the projected graph is emphatically *not* a result of frequent collaborations between productive researchers. Indeed, if we suppose that each of the three papers e_1 , e_2 , and e_3 required the same amount of total effort, the high-degree nodes $A - F$ are the *least* productive nodes in the data set. The high correlation coefficient is driven entirely by two factors, both of which are questionable artifacts of the projection process. First, the single hyperedge e_1 sets the degrees of nodes $A - F$ equal to five, despite the fact that it represents a single collaboration. Second, that single edge is effectively weighted 15 times as much as either of the edges e_2 or e_3 in the computation of the correlation coefficient. This example suggests that assortativity coefficients can display counterintuitive behavior on projections of hypergraphs, and that it may be more interpretable in many cases to compute coefficients directly on the hypergraph structure itself. As we will see, the multidimensionality of hypergraphs enables the computation of multiple categories of assortativity measures, each of which carries distinct information about the local network structure.

Polyadic Assortativity Coefficients

We first define a direct generalization of the Spearman correlation coefficient for hypergraphs. For each edge Δ , let U and V be two uniformly random, distinct nodes in Δ . Let $g : N \rightarrow \mathbb{Z}_+$ assign to each node its degree-rank in the data sample studied. To compute the Spearman coefficient we require the following empirical moments:

$$\begin{aligned}\langle g(U) \rangle &= \frac{1}{|E|} \sum_{\Delta \in E} \frac{1}{|\Delta|} \sum_{u \in \Delta} g(u) \\ \langle g(U)^2 \rangle &= \frac{1}{|E|} \sum_{\Delta \in E} \frac{1}{|\Delta|} \sum_{u \in \Delta} g(u)^2 \\ \langle g(U)g(V) \rangle &= \frac{1}{|E|} \sum_{\Delta \in E} \binom{|\Delta|}{2}^{-1} \sum_{u,v \in \Delta} g(u)g(v)\end{aligned}$$

As before, the general correlation coefficient is defined as the ratio of the covariance to the geometric mean of the variances:

$$\rho = \frac{\langle g(U)g(V) \rangle - \langle g(U) \rangle^2}{\langle g(U)^2 \rangle - \langle g(U) \rangle^2}. \quad (2)$$

Note that each of the moments, and therefore ρ itself, reduce correctly in the case that G is itself a graph. We label ρ the *(polyadic) uniform Spearman coefficient* of degree-assortativity, to distinguish it from the coefficients defined in the next section.

Figure 3 compares the polyadic uniform Spearman coefficient to the dyadic Spearman coefficient computed on the projected graph for a selection of data sets (**A**). Several features are striking. First, the relationship between ρ_{proj} and ρ is nonmonotonic. While these measures are to some extent positively correlated, the difference between them may be large. Second, any of the cases $\rho_{\text{proj}} < \rho$, $\rho_{\text{proj}} > \rho$, and $\rho_{\text{proj}} \approx \rho$ are possible. The sign of the difference tracks to some extent the type of data. All three coauthorship networks, for example, have $\rho_{\text{proj}} > \rho$ by large margins, and the two **thread** data sets display similar differences in the coefficients. Third, for some real-world networks, the choice of $\rho_{\text{projected}}$ may lead to conflicting descriptive findings relative to the choice of ρ . A study using projected line-graphs would suggest that the two thread-based data sets are slightly assortative, whereas a study computing on the full hypergraph would find the sets to be somewhat *disassortative*. A line-graph-based study would compute a lower coefficient for Congressional cosponsorship than geology coauthorship, while a hypergraph-based study would invert this relationship.

Generalized Polyadic Assortativity

The uniform Spearman coefficient is just one of many possible correlation coefficients that may be computed on hypergraphs. Define a (possibly random) *choice function* $\alpha : E \rightarrow N^2$ that assigns to each edge Δ a sub-edge of size 2. We will consider three such choices. For convenience, assume that the nodes $\delta_i \in \Delta$ are ordered by degree, so that $d_{\delta_k} \leq d_{\delta_{k-1}} \cdots \leq$

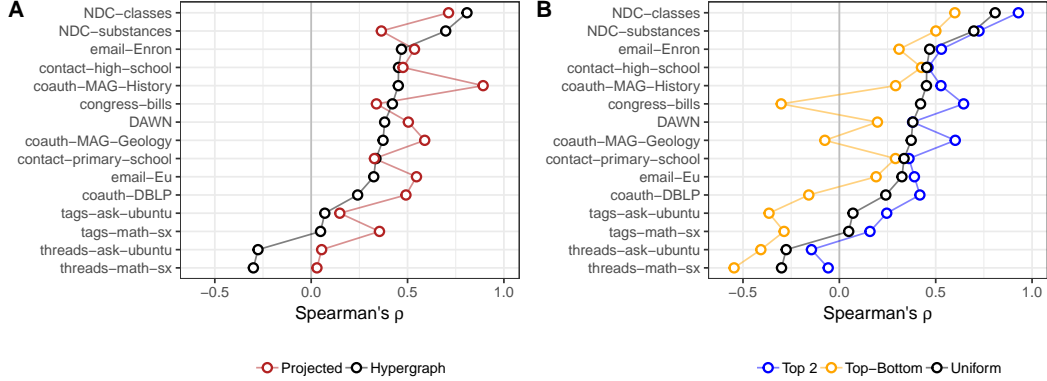


Figure 3: **(A)**: Comparison of Spearman assortativity coefficients computed on the projected graph and the original hypergraph via uniform sampling of nodes on each edge. **(B)**: Comparison of higher-order assortativity coefficients for each data set, computed via the choice functions defined in the main text.

$$d_{\delta_2} \leq d_{\delta_1}.$$

$$\alpha^1(\Delta) \sim \text{unif}\left(\frac{\Delta}{2}\right), \quad (\text{Uniform})$$

$$\alpha^2(\Delta) = (\delta_1, \delta_k), \quad (\text{Top-Bottom})$$

$$\alpha^3(\Delta) = (\delta_1, \delta_2). \quad (\text{Top-2})$$

For any choice function α , we define $h_1 = g \circ \alpha_1$ and $h_2 = g \circ \alpha_2$. The *generalized Spearman assortativity coefficient* with choice function α is

$$\rho_\alpha = \frac{\langle h_1(\Delta)h_2(\Delta) \rangle - \langle h_1(\Delta) \rangle \langle h_2(\Delta) \rangle}{\sqrt{\langle h_1(\Delta)^2 \rangle - \langle h_1(\Delta) \rangle^2} \sqrt{\langle h_2(\Delta)^2 \rangle - \langle h_2(\Delta) \rangle^2}}.$$

In a slight abuse of notation, we have used brackets express averages over both the edges of G and any randomness implicit in α .

The uniform choice function α^1 yields the uniform Spearman coefficient of Equation (2). The choice functions α^2 and α^3 generate novel measures that cannot be nontrivially formulated for binary networks. The resulting coefficients may be used to test a variety of assortativity-related hypotheses in empirical networks. In the case of coauthorship networks, these hypotheses may have the following forms:

1. **Generic Assortativity**: On a given paper, most coauthors will simultaneously be more or less prolific than average.
2. **Junior-Senior Assortativity**: The least prolific author on a paper will tend to be more prolific if the most prolific author is highly prolific.
3. **Senior-Senior Assortativity**: The two most prolific authors on a given paper will tend to be simultaneously more or less prolific than average.

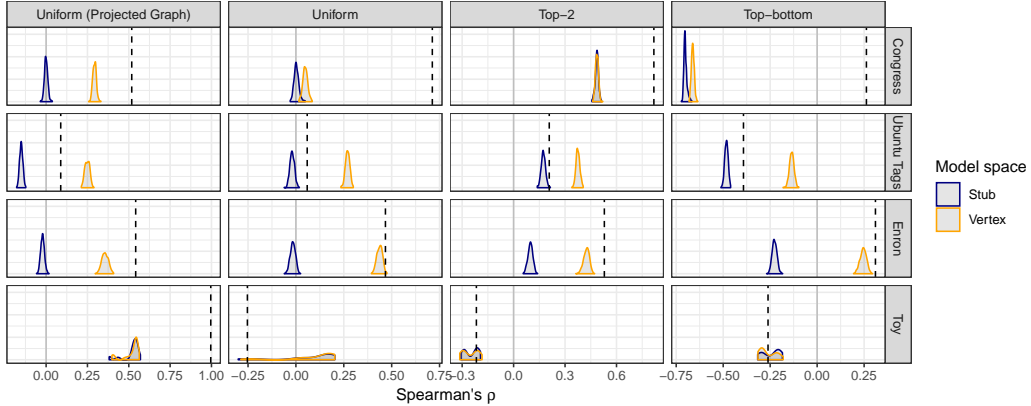


Figure 4: Significance tests for nonrandom assortativity in three empirical networks and the toy synthetic network shown in Figure 2. In each figure, the dashed line gives the observed Spearman correlation, and densities give the null distributions under vertex- and stub-labeled configuration models estimated via Algorithm 1. In the first column only, the network was transformed into the projected graph and the Spearman assortativity was computed via the standard network definition. The second column gives significance tests for the uniform hypergraph Spearman assortativity defined by Equation (2). The third and fourth columns give significance tests for the Top-2 and Top-Bottom assortativity measures. The `congress-bills` and `tags-ask-ubuntu` data sets have been truncated as described in Appendix B.

While the corresponding Spearman coefficients are in general correlated, substantial variation may be observed across our study data sets (Figure 3 (B)). Top-bottom assortativity is especially interesting. By construction it is always less than both the uniform and top-2 measures. The difference, moreover, can be quite large, generating sign-changes in a number of our study data sets. A simple explanation for this phenomenon is the latent influence of edge size. In expectation, the largest degree on an edge is positively correlated with the size of the edge, and the smallest degree negatively so. This influence makes it challenging to interpret Top-2 and Top-Bottom assortativity out of context. While it may be possible to construct alternative numerical measures that account for confounding, a more direct approach is to compare these values to their null distributions under suitably chosen null models.

Hypothesis Tests of Assortativity in Empirical Networks

Not only can degree assortativity measures differ numerically between graph and hypergraph data representations, they can also generate contrasting statistical conclusions. Figure 4 shows a sequence of null hypothesis tests for three empirical networks, alongside the toy network of Figure 2. In each case, we show observed Spearman coefficients alongside their null distributions under both stub- and vertex-labeled configuration models. The first column shows the assortativity computed on the randomized projected graph. This may be directly comparable to the second column in which the assortativity is computed on a randomized hypergraph. In the `congress-bills` data set, randomization under the hyper-

graph configuration model leads to a both a higher uniform assortativity coefficient and a much more significant study finding under both stub- and vertex-labeled models. The `tags-ask-ubuntu` data set illustrates the importance of using null models – while the observed value of ρ is positive, comparison against vertex-labeled nulls shows the network to be significantly *disassortative*. Hypergraph randomization with vertex-labeling leads to a statistically stronger conclusion of disassortativity than randomization of the projected graph. In the `email-Enron` data set, projected and hypergraph null models disagree on the significance of the finding. Vertex-labeled hypergraph randomization suggests that the observed assortativity is consistent with the null hypothesis, while randomization on the projected graph would find the network significantly assortative. Finally, the toy network of Figure 2 is strongly assortative when the projected graph is used in the significance test as described in the main text, but weakly *disassortative* using hypergraph randomization. Not only does the sign of the observed statistic flip, but the directionality of the significance test is also reversed.

The third and fourth columns of Figure 4 illustrate the use of configuration null distributions to evaluate the significance of the Top-2 and Top-Bottom assortativity coefficients, which would otherwise be difficult to assess. In most cases, the tests track the results of the uniform test (second column); however, several interesting features stand out. Despite the fact that Top-Bottom assortativity in the `congress-bills` network is much lower than uniform assortativity, it is much more significant under both labeling schemes. Indeed, the observed uniform assortativity (second column) appears to be driven more by Top-Bottom assortativity (fourth column) than by Top-2 assortativity (third column). In the `email-Enron` network, there are statistically-significant correlations between the Top-2 correspondents on an email and the Top-Bottom correspondents as well. These richer aspects of assortativity are intrinsically polyadic and require hypergraph representations for computation.

These examples illustrate the use of hypergraph null models to provide null distributions for novel metrics. As the example of Figure 2 shows, the choice to project polyadic data to a dyadic graph prior to randomization can play a major role in determining both the available measurements and their appropriate statistical interpretation. Use of hypergraph nulls allows the analyst to forego projection; conduct measurements of degree-assortativity with intuitive properties; compare these measurements to their null distributions; and draw interpretable conclusions.

5.3 Simplicial Closure and the Edge Intersection Profile

Simplicial closure is a recently-observed phenomenon in many empirical polyadic networks [26, 9]. Roughly speaking, simplicial closure refers to the tendency of high-dimensional hyperedges to occur alongside their sub-edges at higher rates than would be expected by chance. Simplicial closure is an example of a phenomenon that requires a higher-order approach to study – indeed, the notion of “sub-edges” cannot be usefully formulated in the language of dyadic graphs. It is thus a ripe topic for study via random hypergraphs.

To illustrate the basic phenomenon, consider the following toy-data set:

$$\{\{A, B\}, \{B, C\}, \{A, C\}, \{A, B, C\}\}. \quad (3)$$

These data *prima facie* exhibit simplicial closure, since the presence of the 3-edge $\{A, B, C\}$ coincides with the presence of each of its sub-edges. The authors of [9] focus on a time-directed notion of simplicial closure, in which we would expect edge $\{A, B, C\}$ to occur after the three sub-edges.

	\bar{T}	Vertex	Stub
email-Enron	0.809	0.218	0.267
email-Eu*	0.741	0.145	0.170
NDC-substances*	0.653	0.141	0.515
NDC-classes*	0.924	0.127	0.140
congress-bills*	0.267	0.071	0.080
coauth-MAG-Geology*	<i>0.996</i>	1.000	1.000

Table 2: Closure of triangles in selected data sets. \bar{T} is the observed proportion of distinct 3-edges to the number of distinct triangles (3-cycles). The observed value may be compared to the values when randomized under vertex- and stub-labeled configuration models in the second and third columns. The standard deviation is less than 0.001 in all null distributions studied. Starred data sets have been temporally subsetting as described in Appendix B.

The authors of [26] measure simplicial closure metric as the ratio of distinct 3-cycles (closed paths of length 3) in the original hypergraph to 2-simplices (i.e. edges with three nodes) in the reduced simplicial complex. A cycle corresponds to a set of three pairwise interactions between three authors, while a 2-simplex corresponds to a joint collaboration between the three of them. The ratio is small when most 3-cycles are “filled in” by three-way collaborations, as illustrated by the toy data above. As a first application of hypergraph nulls to simplicial closure, we study a slightly more general metric, the percentage of 3-cycles which occur as a (not necessarily proper) subset of a higher-dimensional edge. Table 2 displays the empirical value of this measure in a selection of data sets, as well as the summary statistics of the null distributions under vertex and stub-labeling. The `coauth-MAG-Geology` data set displays a slightly but significantly lower rate of filled in triangles than would be expected under either null model. In each of the other data sets studied, triangles are filled in at rates around two-to-five times as frequently as would be expected by chance under either model.

How can we measure simplicial closure of higher-dimensional edges? One approach is to consider the rate of k -cliques occurring as sub-edges. This approach is somewhat inflexible, since a single missing edge from a clique would result in that structure not being counted. Motivated by these considerations, we formulate a simple measure of simplicial closure that is both scalable and flexible.

Definition 12. *The $k\ell$ conditional intersection profile of graph G is the empirical distribution of the intersection size of hyperedges of sizes k and ℓ :*

$$r_{k\ell}(j) = \langle \mathbb{I}(|\Delta \cap \Gamma| = j) \rangle_{k\ell},$$

where $\langle \cdot \rangle_{k\ell}$ denotes the empirical average over all hyperedges Δ of size k and Γ of size ℓ and \mathbb{I} is the indicator function of its argument. The (marginal) intersection profile is

$$r(j) = \langle \mathbb{I}(|\Delta \cap \Gamma| = j) \rangle,$$

with the average taken over all edges in G .

Large values of $r_{k\ell}(j)$ indicate that edges of sizes k and ℓ frequently have intersections of size j . In the toy data given in Equation (3), $r_{23}(2) = 1$, indicating that all 2-edges

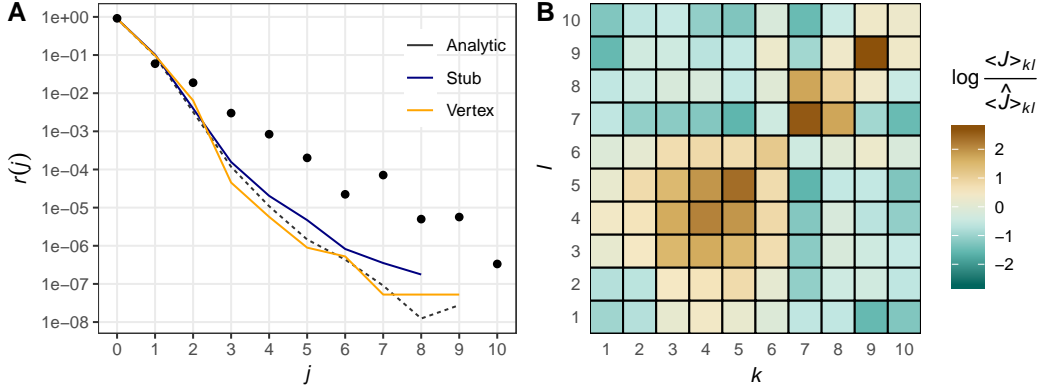


Figure 5: Intersection analysis of the **email-Enron** data set via hypergraph configuration models. **(A)**: Global intersection distribution (points) of the empirical data, compared to null distributions under the stub- and vertex-labeled configuration models. The dashed grey line gives the analytic approximation of Theorem 3. Note the logarithmic vertical axis. **(B)**: The average of the intersection size normalized by the expectation $\langle \hat{J} \rangle_{kl}$ under the vertex-labeled configuration model. Positive values indicate that the data displays larger intersections than expected under the configuration model for the corresponding values of k and l . Colors are shown on a log scale.

are contained in a 3-edge and all 3-edges contain a 2-edge. Data sets of practical interest may possess complex patterns of correlation between simplices of various sizes. Evaluating whether an observed value of $r_{k\ell}(j)$ or $r(j)$ is “large” or not requires comparison to an appropriately-chosen baseline. Such a baseline may be provided by hypergraph configuration models. We note in passing that neither projected graphs or simplicial complexes can be used to study the intersection distribution, since the former contains no sub-edges and the latter by definition contains all of them.

Figure 5 demonstrates the use of hypergraph configuration models in studying the intersection profile of the **email-Enron** data set. The marginal intersection distribution **(A)** is roughly linear on semilog axes, and therefore decays approximately exponentially in j . In order to evaluate whether such behavior is “typical” for graphs sharing the given degree sequence, we turn to hypergraph configuration models. For $j \geq 3$, both the stub- and vertex-labeled models predict mean values of $r(j)$ at least one order of magnitude below what is observed, suggesting the presence of significant local clustering of interactions over and above random chance. The stub- and vertex-labeled models agree directionally with each other and with the analytic approximation of Theorem 3 below.

Further detail on the intersection distribution can be obtained by considering the expected intersection size conditioned on the hyperedge sizes k and l , shown in **(B)**. For each value of k and l , we compute the average size $\langle J \rangle_{kl}$ of the intersection between edges of k and l . We may then compute the same quantity under the vertex-labeled null and compare. Several features of the data structure are illuminated by the heatmap **(B)**. First, the observed averages are not uniformly higher than the null model averages, even on the diagonal. Some combinations of edge-sizes (e.g. edges of size 3 and size 8) actually intersect *less* than would be expected by chance. Second, we observe a tendency of 3-edges to interact with edges of sizes 1-5 more strongly than would be expected at random, corroborating the

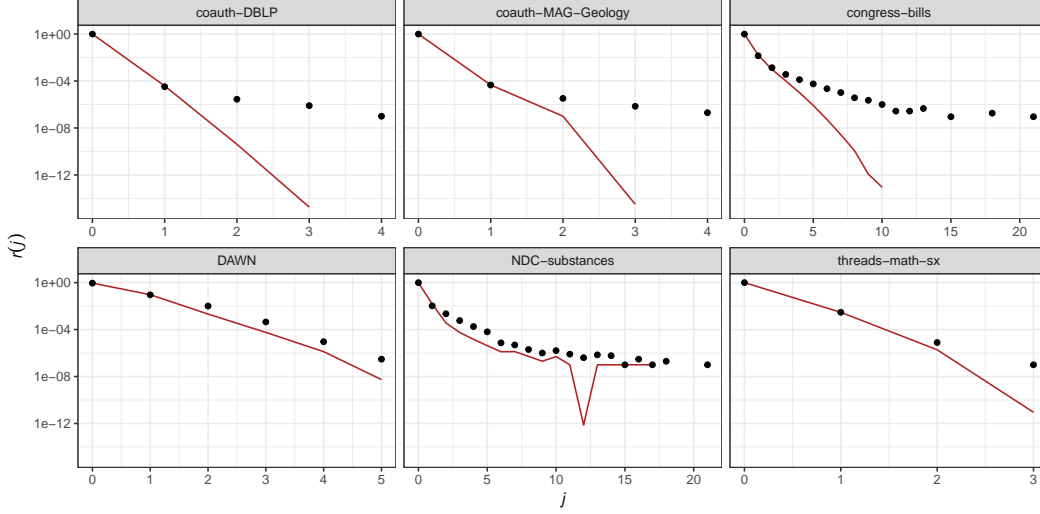


Figure 6: Intersection profiles of large data sets. The solid line gives the approximation provided by Theorem 3. Note the logarithmic vertical axis.

results on closure of triangles studied above. Third, block structure is observable by size: email groupings of sizes 3-6 interact strongly with each other, but not with groupings of larger sizes. Similarly, groupings of sizes 7 and 8 tend to interact strongly with each other, but weakly with smaller sizes.

Approximate Null Intersection Distributions for Large Hypergraphs

For very large graphs, direct Monte Carlo sampling from configuration models may be impractical due to prohibitively long mixing times. For such cases, the following theorem provides a useful approximation to the intersection distribution under the stub-labeled configuration model.

Theorem 3. *Let $\mathbf{D} \in \mathbb{Z}_+^n$ be a vector of i.i.d. copies of random variable D with $\mathbb{E}[D] = \mu_1$ and $\mathbb{E}[D^2] = \mu_2$. Let $\mathbf{K} \in \mathbb{Z}_+^m$ be a vector of edge dimensions configurable with \mathbf{D} . Let $G \sim \eta_{\mathbf{D}, \mathbf{K}}^S$ be distributed according to the stub-labeled configuration model with degree sequence \mathbf{D} and edge-dimensions \mathbf{K} . Let Δ and Γ be uniformly random edges of G . Then, with high probability as n grows large,*

$$r_{k\ell}(j) = (1 + O(n^{-1}))j! \binom{k}{j} \binom{\ell}{j} \left(\frac{1}{n} \frac{\mu_2 - \mu_1}{\mu_1^2} \right)^j$$

The proof of Theorem 3 is provided in Appendix C. In practice, μ_1 and μ_2 may be approximated as empirical averages over the observed degree distribution. The approximation for the **email-Enron** data set is given by the dashed line in Figure 5, and seen to agree quite closely with both the stub- and vertex-labeled nulls.

The utility of Theorem 3 is that only the easily-computed first and second moments of the degree distribution are required, allowing the analyst to completely bypass simulation if required. Figure 5 (A) visualizes the approximation alongside the distributions computed

via stub- and vertex-labeled sampling, finding the agreement to be excellent across many orders of magnitude with both the stub- and vertex-labeled configuration models. We therefore use this approximation to study the higher-order organization of networks for which explicit Monte Carlo randomization may not be practical. Figure 6 compares the observed and approximate intersection distributions for a range of larger data sets.

The data display a range of behaviors. Some, such as `NDC-substances` and `DAWN` follow the approximation quite closely, and may therefore be viewed as near-random random with respect to intersections. Other data sets significantly deviate from the approximate null values, with heavy tails, indicating strong polyadic correlation of edges. The `congress-bills` data set is of special interest. There are approximately as many intersections of size 1 and 2 as would be expected under the null, but the tail of the distribution is vastly heavier than would be predicted by chance.

Simplicial closure is an intriguing aspect of many polyadic data sets, the study of which is still in infancy. We have shown here how measurements of simplicial closure may be compared against hypergraph null models, and how the resulting comparisons can shed light on mesoscale structures in the data. We hope that hypergraph nulls will provide support for future studies of simplicial closure and its implications for networked systems.

6 Conclusions

The paradigm of dyadic networks has proven immensely fruitful in the modeling of a vast range of empirical phenomena. The dyadic paradigm, however, has limitations. Researchers are increasingly turning to polyadic models in a variety of scientific domains. The interpretation of measurements on these models requires principled benchmarks in the form of null models. We have developed a class of such null models on the space of hypergraphs, and argued that this space is the natural home of many classical data genres, including collaborations, interactions, and compositions. These models are maximally random distributions subject to preservation of the degree sequence and edge-dimension sequence, and therefore generalize the classical configuration model of network science. Following [25], we defined both stub- and vertex-labeled variants of the model, and developed algorithms for approximate sampling.

We have also considered a sequence of applications. These applications underscore the importance of data representations in both *computing* metrics and *randomizing* for significance tests. A principal theme has been the importance of randomizing in the “native space” of the data, prior to projections and other transformations. When studying triadic clustering in polyadic networks, we showed that interchanging the projection and randomization operations leads to dramatically differing conclusions about the prevalence of nonrandom clustering in real-world data sets. Degree-assortativity has typically been studied by computing correlations on the projected graph. We argued that working on the projected graph can distort both our intuition about the meaning of assortativity and the statistical significance of the resulting measurements. Finally, the study of simplicial closure and simplicial clustering in polyadic networks intrinsically requires polyadic measures. We developed an intuitive measure of simplicial closure – the intersection profile – and showed how to use this measure to study the degree of edge-edge correlations in empirical data sets. We also developed an analytic approximation to the null profile which can be used to analyze data sets of arbitrary size.

There are several promising directions of future research in configuration models of ran-

dom hypergraphs. Theorem 3, describing the asymptotic intersection profile in stub-labeled configuration models, suggests the possibility of analytic approximations to other important model moments. Also intriguing is the possibility of using hypergraph configuration models for the construction of modularity functions for community detection. The work of [20] shows several methods for doing this via a hypergraph Chung-Lu model. Lemma 2 implies that the stub-labeled configuration model gives asymptotically equivalent marginal expectations within the modularity function. However, many empirical polyadic networks are more appropriately studied via the vertex-labeled model, for which we possess no analogue of Lemma 2. To perform vertex-labeled community detection, it is therefore necessary to estimate the relevant marginal expectations, a task which may pose interesting probabilistic and statistical challenges. It is our hope that these and other developments will contribute to the emerging landscape of polyadic network analysis.

Acknowledgements

I am grateful to Patrick Jaillet for helpful discussions, and to the National Science Foundation for support under Graduate Research Fellowship Grant 1122374.

References

- [1] Juliette Stehlé, Nicolas Voirin, Alain Barrat, Ciro Cattuto, Lorenzo Isella, Jean François Pinton, Marco Quaggiotto, Wouter van den Broeck, Corinne Régis, Bruno Lina, and Philippe Vanhems. High-resolution measurements of face-to-face contact patterns in a primary school. *PLoS ONE*, 6(8), 2011.
- [2] Rossana Mastrandrea, Julie Fournet, and Alain Barrat. Contact patterns in a high school: A comparison between data collected using wearable sensors, contact diaries and friendship surveys, 2015.
- [3] Mark E. J. Newman. Scientific collaboration networks. II. Shortest paths, weighted networks, and centrality. *Physical Review E - Statistical Physics, Plasmas, Fluids, and Related Interdisciplinary Topics*, 64(1):7, 2001.
- [4] Mark E. J. Newman. Scientific collaboration networks. I. Network construction and fundamental results. *Physical Review E - Statistical Physics, Plasmas, Fluids, and Related Interdisciplinary Topics*, 64(1):8, 2001.
- [5] Albert-Laszlo Barabasi, Hawoong Jeong, Z. Neda, E. Ravasz, A. Schubert, and T. Vicsek. Evolution of the social network of scientific collaborations. *Physica A: Statistical Mechanics and its Applications*, 311(3-4):590–614, 2002.
- [6] James H Fowler. Legislative cosponsorship networks in the US House and Senate. *Social Networks*, 28:454–465, 2006.
- [7] Mason A Porter, Peter J Mucha, M E J Newman, and Casey M Warmbrand. A network analysis of committees in the U. S. House of Representatives. *Proceedings of the National Academy of Sciences*, 102(20):7057–7062, 2005.
- [8] Bryan Klimt and Yiming Yang. Introducing the Enron Corpus. In *CEAS*, 2004.

- [9] Austin R. Benson, Rediet Abebe, Michael T. Schaub, Ali Jadbabaie, and Jon Kleinberg. Simplicial Closure and Higher-order Link Prediction. *Proceedings of the National Academy of Sciences*, 115(48):11221–11230, 2018.
- [10] Hyejin Youn, Deborah Strumsky, Luis M. A. Bettencourt, and José Lobo. Invention as a combinatorial process: evidence from US patents. *Journal of the Royal Society, Interface*, 12(106):20150272–, 2015.
- [11] Chad Giusti, Robert Ghrist, and Danielle S. Bassett. Two’s company, three (or more) is a simplex: Algebraic-topological tools for understanding higher-order structure in neural data. *Journal of Computational Neuroscience*, 41(1):1–14, 2016.
- [12] Jacopo Grilli, György Barabás, Matthew J. Michalska-Smith, and Stefano Allesina. Higher-order interactions stabilize dynamics in competitive network models. *Nature*, 2017.
- [13] J. Ugander, L. Backstrom, C. Marlow, and J. Kleinberg. Structural diversity in social contagion. *Proceedings of the National Academy of Sciences*, 109(16):5962–5966, 2012.
- [14] Austin R. Benson, David F. Gleich, and Jure Leskovec. Higher-Order Organization of Complex Networks. *Science*, 353(6295):163–166, 2016.
- [15] Michael T Schaub, Austin R Benson, Paul Horn, Gabor Lippner, and Ali Jadbabaie. Random Walks on Simplicial Complexes and the normalized Hodge Laplacian. 2018.
- [16] Béla Bollobás. A Probabilistic Proof of an Asymptotic Formula for the Number of Labelled Regular Graphs. *European Journal of Combinatorics*, 1(4):311–316, 1980.
- [17] Michael Molloy and Bruce Reed. The Size of the Giant Component of a Random Graph with a Given Degree Sequence. *Combinatorics, Probability, and Computing*, 7(3):295–305, 1998.
- [18] Gourab Ghoshal, Vinko Zlatić, Guido Caldarelli, and Mark E. J. Newman. Random hypergraphs and their applications. *Physical Review E - Statistical, Nonlinear, and Soft Matter Physics*, 2009.
- [19] Tarun Kumar, Sankaran Vaidyanathan, Harini Ananthapadmanabhan, Srinivasan Parthasarathy, and Balaraman Ravindran. Hypergraph Clustering: A Modularity Maximization Approach. 2018.
- [20] Bogumil Kaminski, Valerie Poulin, Pawel Pralat, Przemyslaw Szufel, and Francois Theberge. Clustering via Hypergraph Modularity. pages 1–17, 2018.
- [21] Mark E. J. Newman, S. H. Strogatz, and D. J. Watts. Random graphs with arbitrary degree distributions and their applications. *Physical Review E - Statistical Physics, Plasmas, Fluids, and Related Interdisciplinary Topics*, 64(2):17, 2001.
- [22] Fabio Saracco, Riccardo Di Clemente, Andrea Gabrielli, and Tiziano Squartini. Randomizing bipartite networks: the case of the World Trade Web. *Scientific Reports*, 5(10595):1–18, 2015.
- [23] Jean Gabriel Young, Giovanni Petri, Francesco Vaccarino, and Alice Patania. Construction of and efficient sampling from the simplicial configuration model. *Physical Review E*, 96(3):1–6, 2017.

- [24] Owen T. Courtney and Ginestra Bianconi. Generalized network structures: The configuration model and the canonical ensemble of simplicial complexes. *Physical Review E*, 93(6):1–26, 2016.
- [25] Bailey K Fosdick, Daniel B Larremore, Joel Nishimura, and Johan Ugander. Configuring random graph models with fixed degree sequences. *SIAM Review*, 60(2):315–355, 2018.
- [26] Alice Patania, Giovanni Petri, and Francesco Vaccarino. The shape of collaborations. *EPJ Data Science*, 6(1):1–16, 2017.
- [27] M E J Newman. Modularity and community structure in networks. *Proceedings of the National Academy of Sciences*, 103(23):8577–8582, 2006.
- [28] Santo Fortunato and Marc Barthélemy. Resolution limit in community detection. *Proceedings of the National Academy of Sciences*, 104(1):36–41, 2006.
- [29] Gunnar Carlsson. Topology and data. *Bulletin of the American Mathematical Society*, 46(2):255–308, 2009.
- [30] Diamantino C da Silva, Ginestra Bianconi, Rui A da Costa, Sergey N Dorogovtsev, and José FF Mendes. Complex network view of evolving manifolds. *Physical Review E*, 97(3):032316, 2018.
- [31] Ginestra Bianconi and Christoph Rahmede. Emergent hyperbolic geometry of growing simplicial complexes. (July), 2016.
- [32] Owen T. Courtney and Ginestra Bianconi. Weighted growing simplicial complexes. *Physical Review E*, 2017.
- [33] Zhihao Wu, Giulia Menichetti, Christoph Rahmede, and Ginestra Bianconi. Emergent complex network geometry. *Scientific Reports*, 5, 2015.
- [34] A. Costa and M. Farber. Large random simplicial complexes, I. *Journal of Topology and Analysis*, 08(03):399–429, 2016.
- [35] A Costa and M Farber. Random simplicial complexes. In *Configuration Spaces*, pages 129–153. 2016.
- [36] Ann E. Sizemore, Jennifer Phillips-Cremins, Robert Ghrist, and Danielle S. Bassett. The importance of the whole: topological data analysis for the network neuroscientist. *arXiv:1806.05167*, 2018.
- [37] Ernesto Estrada and Grant Ross. Centralities in Simplicial Complexes. *arXiv:1703.03641*, 2017.
- [38] Fan Chung and Linyuan Lu. Connected components in random graphs with given expected degree sequences. *Annals of combinatorics*, 6(2):125–145, 2002.
- [39] S. H. Strogatz and D. J. Watts. Collective dynamics of 'small-world' networks. *Nature*, 393(June):440–442, 1998.
- [40] Hao Yin, Austin R. Benson, and Jure Leskovec. Higher-order clustering in networks. *Physical Review E*, 97(5), 2018.

- [41] Mark E. J. Newman. *Networks: An Introduction*. Oxford University Press, 2010.
- [42] James Moody. Race, school integration, and friendship segregation in america. *American journal of Sociology*, 107(3):679–716, 2001.
- [43] Mark E. J. Newman. Mixing patterns in networks. *Physical Review E - Statistical Physics, Plasmas, Fluids, and Related Interdisciplinary Topics*, 67(2):13, 2003.
- [44] Mark E. J. Newman. Assortative Mixing in Networks. *Physical Review Letters*, 89(20):1–5, 2002.
- [45] V. Colizza, A. Flammini, M. A. Serrano, and A. Vespignani. Detecting rich-club ordering in complex networks. *Nature Physics*, 2(2):110–115, 2006.
- [46] Remco van der Hofstad and Nelly Litvak. Degree-degree dependencies in random graphs with heavy-tailed degrees. *Internet Mathematics*, 10(3-4):287–334, 2014.
- [47] James H. Fowler. Connecting the congress: A study of cosponsorship networks. *Political Analysis*, 14(04):456–487, 2006.
- [48] Arnab Sinha, Zhihong Shen, Yang Song, Hao Ma, Darrin Eide, Bo-June (Paul) Hsu, and Kuansan Wang. An overview of microsoft academic service (MAS) and applications. In *Proceedings of the 24th International Conference on World Wide Web*. ACM Press, 2015.
- [49] Omer Angel, Remco van der Hofstad, and Cecilia Holmgren. Limit laws for self-loops and multiple edges in the configuration model. *arXiv preprint*, 2016.
- [50] David Aldous. *Probability approximations via the Poisson clumping heuristic*. Springer Science and Business Media, 2013.

Appendix A Software

An implementation of a the vertex- and stub-labeled null models for random hypergraphs is available at <https://github.com/PhilChodrow/hypergraph>.

Appendix B Data Preparation

The data used for examples in this paper were prepared by the authors of [9] and accessed from <https://www.cs.cornell.edu/~arb/data/>. Some data sets have been subsetted via a temporal threshold in order to promote practical compute times on clustering, triangle counting, and mixing of vertex-labeled models in projected graph spaces. Notably, in no cases was the limiting factor on compute times mixing on hypergraph spaces. Thresholds were chosen to construct data of approximate order $m \approx 10^4$, but are otherwise arbitrary. Temporal data subsets were used in the generation of Tables 1 and 2 and fig. 4. Table 3 gives the node and edge counts of both the original data and the data after temporal subsetting when applicable.

	Original		t	Filtered	
	n	m		n	m
email-Enron	149	10,886	–	–	–
email-Eu	1,006	235,264	1.105×10^9	817	32,117
congress-bills [47, 6]	1,719	260,852	7.315×10^5	537	6,661
coauth-MAG-Geology [48]	1,261,130	1,591,167	2017	73,436	23,434
coauth-DBLP	1,930,379	3,700,682	–	–	–
NDC-classes	1,162	49,727	6.3554192×10^{13}	815	9,787
NDC-substances	5,557	112,920	6.3554192×10^{13}	4502	85,838
tags-math-sx	1,630	822,060	–	–	–
threads-ask-ubuntu	3,030	271,234	–	–	–
threads-math-sx	201,864	719,793	2.19×10^{12}	11,880	22,786
tags-ask-ubuntu	200,975	192,948	2.6×10^{12}	2,120	19,338
DAWN	2,558	2,272,434	–	–	–
contact-primary-school	242	106,880	–	–	–
contact-primary-school	327	172,036	–	–	–

Table 3: Summary of data preparation.

Appendix C Proof of Theorem 3

While some technical steps are required in order to prove this result, the intuition is relatively simple. Consider an urn in which there are d_u copies of each node u . Suppose we choose two copies C_1 and C_2 from the urn. The probability that the two copies are identical is

$$\begin{aligned}
q &= \mathbb{P}(C_1 = C_2) \\
&= \sum_{u \in N} \mathbb{P}(C_1 = u) \mathbb{P}(C_2 = u | C_1 = u) \\
&= \sum_{u \in N} \frac{d_u}{\sigma_1(\mathbf{d})} \frac{d_u - 1}{\sigma_1(\mathbf{d}) - 1} \\
&\approx \frac{1}{n\mu_1(n\mu_1 - 1)} n(\mu_2 - \mu_1) \\
&= (1 + O(n^{-1})) \frac{1}{n} \frac{\mu_2 - \mu_1}{\mu_1^2}.
\end{aligned}$$

The approximation reflects concentration of empirical averages to expectations, and can be made precise via the CLT. The event $J = j$ is composed of j such matches. There are $\binom{k}{j}$ ways to choose the j matching nodes from the first edge, and $\binom{\ell}{j}$ ways to choose the j matching nodes from the second. There are then $j!$ distinct ways to place the matching nodes from each edge in corresponding with each other.

Algorithm 2 Stub-Matching for $\eta_{\mathbf{d},\mathbf{k}}^\ell$

Data: Degree sequence \mathbf{d} , hyperedge dimension sequence \mathbf{k} .

Result: \mathcal{G} , a (possibly degenerate) hypergraph with degree sequence \mathbf{d} and hyperedge dimension sequence \mathbf{k}

Initialization:

$j \leftarrow 1$

$\mathcal{G} \leftarrow \emptyset$

$W \leftarrow \bigcup_{i=1}^n W_i$, where each W_i is a set of d_i labeled stubs associated with node i .

while $j \leq n$ **do**

 Sample set R uniformly without replacement from W , with $|R| = k_j$.

$W \leftarrow W \setminus R$

$\mathcal{G} \leftarrow \mathcal{G} \cup \{R\}$.

$j \leftarrow j + 1$

end

return \mathcal{G}

C.1 Generalized Stub Matching for Stub-Labeled Hypergraphs

Stub-matching was famously introduced by [16] as a method for approximately counting the number of regular random graphs, stub-matching offers an intuitive construction of uniform samples from the network configuration model. Furthermore, after nearly forty years of development, the probabilistic theory of stub-matching is by now rich and relatively well-understood, with Poissonian limit laws in place for many quantities of algorithmic interest [49, 50].

The generalization of stub-matching to stub-labeled hypergraphs is straightforward. Stub-matching for this model exactly follows the original construction of [16], except instead of partitioning the set of labeled stubs into pairs, we partition it into sets of heterogeneous size governed by \mathbf{k} . The algorithm is formalized in Algorithm 2. The return value of Algorithm 2 may be a *degenerate* hypergraph containing one or more edges in which a single node is repeated twice. Such degenerate edges are the hypergraph generalization of self-loops, and are not elements of $\mathcal{S}_{\mathbf{d},\mathbf{k}}$. As a result, Algorithm 2 has a nonzero probability to fail. Conditioned on the production of a nondegenerate hypergraph, however, Algorithm 2 is indeed a correct algorithm for sampling from $\eta_{\mathbf{d},\mathbf{k}}^S$.

Theorem 4. *Let μ_{sm} be the probability measure over hypergraphs defined by Algorithm 2. Let $B(G)$ be the event that G is nondegenerate. Then,*

$$\eta_{\mathbf{d},\mathbf{k}}^S(G) = \mu_{\text{sm}}(G|B(G)).$$

Proof. We note that Algorithm 2 is equally likely to produce any (possibly degenerate) matching of stubs, implying that μ_{sm} is uniform on the space of degenerate hypergraphs with degree sequence \mathbf{d} and dimension sequence \mathbf{k} . The conditional distribution $\mu_{\text{sm}}(\cdot|B(G))$ is again uniform on the space of nondegenerate hypergraphs with the specified degree and dimension sequences. But that space is simply $\mathcal{S}_{\mathbf{d},\mathbf{k}}$, and $\mu_{\text{sm}}(\cdot|B(G))$ is therefore identical to $\eta_{\mathbf{d},\mathbf{k}}^S$, as was to be shown. \square

C.2 Proof of Theorem 3

Theorem 4 enables us to provide an approximation for the marginal distribution of a single hyperedge in the stub-labeled configuration model, conditioned on its size. For our approximations we employ zeroth-order asymptotics:

Definition 13 (Zeroth-Order Asymptotics). *Functions f and g of n are zeroth-order equivalent if $f(n) = g(n) (1 + O(n^{-1}))$ with high probability as n grows large. In this case, we write $f(n) \doteq g(n)$.*

This definition implies that the absolute error when using f to approximate g decays at least as n^{-1} . It is also convenient to introduce the elementary symmetric polynomials:

$$\sigma_k(\mathbf{v}) \triangleq \sum_{R \in \binom{[v]}{k}} \prod_{r \in R} v_r .$$

Lemma 2. *Let Δ be a fixed hyperedge of $G \sim \eta_{\mathbf{d}, \mathbf{k}}^S$. Then,*

$$\eta_{\mathbf{d}, \mathbf{k}}^S(\Delta = R \mid |\Delta| = q) \doteq \begin{cases} \frac{k! \sigma_k(\mathbf{d}_R)^k}{\sigma_1(\mathbf{d})^k} & |R| = k \\ 0 & \text{otherwise} . \end{cases}$$

Proof. Consider the stub-matching algorithm, and suppose without loss of generality that Δ is the first hyperedge placed. First, arbitrarily order the elements of Δ as $\delta_1, \dots, \delta_k$ and the elements of R as r_1, \dots, r_k . There are a total of $\sigma_1(\mathbf{d})$ stubs, and of these d_{r_1} are attached to node r_1 . Stub-matching thus sets $\delta_1 = r_1$ with probability $\frac{d_{r_1}}{\sigma_1(\mathbf{d})}$. For δ_2 , there are $\sigma_1(\mathbf{d}) - d_{r_1}$ stubs remaining, and of these d_{r_2} are attached to node r_2 , giving the event $\delta_2 = r_2$ (conditional on $\delta_1 = r_1$) with probability $\frac{d_{r_2}}{\sigma_1(\mathbf{d}) - d_{r_1}}$. Continuing inductively, we have

$$\eta(\delta_1 = r_1, \dots, \delta_k = r_k) = \prod_{i=1}^k \frac{d_{r_i}}{\sigma_1(\mathbf{D}) - \sum_{\ell=1}^{i-1} d_{r_\ell}} .$$

It is convenient to expand and simplify the product, obtaining

$$\begin{aligned} \eta(\delta_1 = r_1, \dots, \delta_k = r_k) &= \frac{\sigma_k(\mathbf{d}_R)}{\sigma_1(\mathbf{d})^k} \prod_{i=1}^k \frac{1}{1 - \sigma_1(\mathbf{D})^{-1} \sum_{\ell=1}^{i-1} d_{r_\ell}} \\ &= \frac{\sigma_k(\mathbf{d}_R)}{\sigma_1(\mathbf{d})^k} \prod_{i=1}^k \left[1 + \sigma_1(\mathbf{d})^{-1} \sum_{\ell=1}^{i-1} d_{r_\ell} + O((\sigma_1(\mathbf{d})^{-1} \sum_{\ell=1}^{i-1} d_{r_\ell})^2) \right] \\ &= \frac{\sigma_k(\mathbf{d}_R)}{\sigma_1(\mathbf{d})^k} \prod_{i=1}^k [1 + O(n^{-1})] \\ &\doteq \frac{\sigma_k(\mathbf{d}_R)}{\sigma_1(\mathbf{d})^k} . \end{aligned}$$

There are $k!$ ways to place the elements of Δ and R in correspondence, each of which has probability approximately given by the final line. Multiplying through by this factor of $k!$ completes the proof. \square

We may now calculate the expected value of $r_{k\ell}(j)$ under the conditions of Theorem 3. Recall that the expectation is taken over realizations of the degree sequence \mathbf{D} , which is a sequence of i.i.d. copies of random variable D with first moment μ_1 and second moment μ_2 .

Lemma 3. *We have*

$$\mathbb{E}_D[r_{k\ell}(j)] \doteq j! \binom{k}{j} \binom{\ell}{j} \left(\frac{1}{n} \frac{\mu_2 - \mu_1}{\mu_1^2} \right)^j.$$

Proof. We begin by conditioning over the location of the intersection. For notational simplicity, we will $|\Delta| = k$ and $|\Gamma| = j$ and drop the explicit conditioning on these events. There are $\binom{k}{j}$ ways to choose the nodes of Δ that participate in the intersection, and $\binom{\ell}{j}$ ways to choose the nodes of Γ . There are then $j!^2$ ways to order both sets of nodes. Pick one such ordering, and define the event

$$A_j = \{\delta_1 = \gamma_1, \dots, \delta_j = \gamma_j\} \cap \{|\Delta \cap \Gamma| = j\}.$$

Then,

$$\eta(|\Delta \cap \Gamma| = j) = j! \binom{k}{j} \binom{\ell}{j} \eta(A_j).$$

We will show that $\eta(A_j) \doteq \frac{1}{j!} \left(\frac{1}{n} \frac{\mu_2 - \mu_1}{\mu_1^2} \right)^j$, from which the result will follow. Conditioning explicitly and employing Lemma 2, we have

$$\eta(A_j) \doteq \sum_{R \in \binom{N}{j}} \left(\frac{\sigma_j(\mathbf{D}_R) \sigma_j(\mathbf{D}_R - \mathbf{e}_R)}{\sigma_1(\mathbf{D})^j \sigma_1(\mathbf{D} - \mathbf{e}_R)^j} \right) \sum_{S \in \binom{N \setminus R}{k-j}} \frac{\sigma_{k-j}(\mathbf{D}_S)}{\sigma_1(\mathbf{D} - 2\mathbf{e}_R)^{k-j}} \sum_{T \in \binom{N \setminus (R \cup T)}{\ell-j}} \frac{\sigma_{\ell-j}(\mathbf{D}_T)}{\sigma_1(\mathbf{D} - 2\mathbf{e}_R - \mathbf{e}_S)^{\ell-j}}.$$

The first factor sums over possible locations of the intersection. The second sums over possible locations of the remaining $k-j$ elements of Δ , and the third over the remaining $\ell-j$ elements of Γ . Via standard Taylor expansions, all the denominators are zeroth-order equivalent to powers of $\sigma_1(\mathbf{D})$:

$$\eta(A_j) \doteq \frac{1}{\sigma_1(\mathbf{D})^{k+\ell}} \sum_{R \in \binom{N}{j}} \sigma_j(\mathbf{D}_R) \sigma_j(\mathbf{D}_R - \mathbf{e}_R) \sum_{S \in \binom{N \setminus R}{k-j}} \sigma_{k-j}(\mathbf{D}_S) \sum_{T \in \binom{N \setminus (R \cup T)}{\ell-j}} \sigma_{\ell-j}(\mathbf{D}_T).$$

The two inner sums may be consolidated. Each term within the inner two sums contains $k + \ell - 2j$ distinct elements of \mathbf{D}_{R^c} , with all combinations present. We therefore have

$$\sum_{S \in \binom{N \setminus R}{k-j}} \sigma_{k-j}(\mathbf{D}_S) \sum_{T \in \binom{N \setminus (R \cup T)}{\ell-j}} \sigma_{\ell-j}(\mathbf{D}_T) = \sigma_{k+\ell-2j}(\mathbf{D}_{R^c}).$$

Since only a finite number of elements of \mathbf{D} are missing from the degree sequence in this expression, we further have that

$$\sigma_{k+\ell-2j}(\mathbf{D}_{R^c}) \doteq \sigma_{k+\ell-2j}(\mathbf{D}).$$

Consolidating,

$$\eta(A_j) \doteq \left(\frac{1}{\sigma_1(\mathbf{D})^{2j}} \sum_{R \in \binom{N}{j}} \sigma_j(\mathbf{D}_R) \sigma_j(\mathbf{D}_R - \mathbf{e}_R) \right) \frac{\sigma_{k+\ell-2j}(\mathbf{D})}{\sigma_1(\mathbf{D})^{k+\ell-2j}}.$$

In the second factor, the numerator and denominator have the same leading terms and are therefore zeroth-order equivalent. Focusing on the first factor, we note that $\sigma_1(\mathbf{D}) \doteq \sigma_1(\mathbf{D}_{R^c})$, again since only finitely many terms are missing in the second factor. Using this fact and computing expectations over \mathbf{D} , we have

$$\begin{aligned} \mathbb{E}[\eta(A_j)] &\doteq \mathbb{E} \left[\frac{1}{\sigma_1(\mathbf{D})^{2j}} \sum_{R \in \binom{N}{j}} \sigma_j(\mathbf{D}_R) \sigma_j(\mathbf{D}_R - \mathbf{e}_R) \right] \\ &\doteq \mathbb{E} \left[\sum_{R \in \binom{N}{j}} \frac{\sigma_j(\mathbf{D}_R) \sigma_j(\mathbf{D}_R - \mathbf{e}_R)}{\sigma_1(\mathbf{D}_{R^c})^{2j}} \right] \\ &= \sum_{R \in \binom{N}{j}} \mathbb{E} \left[\frac{1}{\sigma_1(\mathbf{D}_{R^c})^{2j}} \right] \mathbb{E} [\sigma_j(\mathbf{D}_R) \sigma_j(\mathbf{D}_R - \mathbf{e}_R)] \end{aligned}$$

Via the Central Limit Theorem, the first factor satisfies, for any R ,

$$\mathbb{E} \left[\frac{1}{\sigma_1(\mathbf{D}_{R^c})^{2j}} \right] \doteq \mathbb{E} \left[\frac{1}{\sigma_1(\mathbf{D})^{2j}} \right] \doteq \frac{1}{(n\mu_1)^{2j}}.$$

Similarly, the second factor satisfies for any R

$$\mathbb{E} [\sigma_j(\mathbf{D}_R) \sigma_j(\mathbf{D}_R - \mathbf{e}_R)] \doteq (\mu_2 - \mu_1)^j.$$

Finally, there are $\binom{n}{j} \doteq \frac{n^j}{j!}$ terms in the summation. Consolidating, we have

$$\begin{aligned} \mathbb{E}[\eta(A_j)] &\doteq \frac{1}{(n\mu_1)^{2j}} \frac{n^j}{j!} (\mu_2 - \mu_1)^j \\ &= \frac{1}{j!} \left(\frac{1}{n} \frac{\mu_2 - \mu_1}{\mu_1^2} \right)^j. \end{aligned}$$

This completes the proof. \square

To complete the proof of Theorem 3, we now demonstrate concentration of $r_{k\ell}(j)$ around its expectation. In order to make the dependence on the random vector \mathbf{D} explicit, define $q_j(\mathbf{D}) = \eta_{\mathbf{D}}(A_j)$, and recall that $r_{k\ell}(j) = j!^2 \binom{k}{j} \binom{\ell}{j} q_j(\mathbf{D})$. We will employ the Efron-Stein inequality in order to bound $q_j(\mathbf{D})$. The inequality states that

$$\text{var}(q_j(\mathbf{D})) \leq \frac{1}{2} \sum_{v \in N} \mathbb{E} \left[\left(q_j(\mathbf{D}) - q_j(\mathbf{D}^{(v)}) \right)^2 \right], \quad (4)$$

where $\mathbf{D}^{(v)}$ is the vector \mathbf{D} in which entry D_v has been resampled from the distribution of D . The terms in the summation are often called the *influence* of entry i . Equation (4) is especially well-suited to working with elementary symmetric polynomials, as expressions for the influences within the summation may be computed explicitly.

Proof of Theorem 3. Fix $v \in N$. We begin with the following expression for $\eta(A_j)$:

$$q_j(\mathbf{D}) = \eta(A_j) \doteq \sum_{R \in \binom{N}{j}} \frac{\sigma_j(\mathbf{D}_R) \sigma_j(\mathbf{D}_R - \mathbf{e}_R)}{\sigma_1(\mathbf{D}_{R^c})^{2j}}.$$

We can split the sum according to whether $v \in R$, obtaining

$$q_j(\mathbf{D}) \doteq \mathbf{D}_v(\mathbf{D}_v - 1) \sum_{S \in \binom{N \setminus v}{j-1}} \frac{\sigma_j(\mathbf{D}_S) \sigma_j(\mathbf{D}_S - \mathbf{e}_S)}{\sigma_1(\mathbf{D}_{(S \cup v)^c})^{2j}} + \sum_{R \in \binom{N \setminus v}{j}} \frac{\sigma_j(\mathbf{D}_R) \sigma_j(\mathbf{D}_R - \mathbf{e}_R)}{\sigma_1(\mathbf{D}_{R^c})^{2j}}.$$

Then, since the second term does not depend on \mathbf{D}_v ,

$$q_j(\mathbf{D}) - q_j(\mathbf{D}^{(v)}) \doteq (\mathbf{D}_v(\mathbf{D}_v - 1) - \mathbf{D}'_v(\mathbf{D}'_v - 1)) \sum_{S \in \binom{N \setminus v}{j-1}} \frac{\sigma_j(\mathbf{D}_S) \sigma_j(\mathbf{D}_S - \mathbf{e}_S)}{\sigma_1(\mathbf{D}_{(S \cup v)^c})^{2j}}.$$

Squaring and computing expectations,

$$\mathbb{E} \left[\left(q_j(\mathbf{D}) - q_j(\mathbf{D}^{(v)}) \right)^2 \right] \doteq \mathbb{E} \left[\left(\sum_{S \in \binom{N \setminus v}{j-1}} \frac{\sigma_j(\mathbf{D}_S) \sigma_j(\mathbf{D}_S - \mathbf{e}_S)}{\sigma_1(\mathbf{D}_{(S \cup v)^c})^{2j}} \right)^2 \right] \mathbb{E} \left[(\mathbf{D}_v(\mathbf{D}_v - 1) - \mathbf{D}'_v(\mathbf{D}'_v - 1))^2 \right].$$

The second factor can be computed explicitly:

$$\begin{aligned} \mathbb{E} \left[(\mathbf{D}_v(\mathbf{D}_v - 1) - \mathbf{D}'_v(\mathbf{D}'_v - 1))^2 \right] &= 2\mathbb{E}[\mathbf{D}_v^2(\mathbf{D}_v - 1)^2] - 2\mathbb{E}[\mathbf{D}_v(\mathbf{D}_v - 1)]^2 \\ &= 2(\mu_4 - 2\mu_3 + \mu_2 - (\mu_2 - \mu_1)^2). \end{aligned}$$

It remains to approximate the first factor. In the zeroth-order asymptotics, the denominator factors out and may be computed explicitly.

$$\begin{aligned} \mathbb{E} \left[\left(\sum_{S \in \binom{N \setminus v}{j-1}} \frac{\sigma_j(\mathbf{D}_S) \sigma_j(\mathbf{D}_S - \mathbf{e}_S)}{\sigma_1(\mathbf{D}_{(S \cup v)^c})^{2j}} \right)^2 \right] &\doteq \mathbb{E} \left[\left(\sum_{S \in \binom{N \setminus v}{j-1}} \frac{\sigma_j(\mathbf{D}_S) \sigma_j(\mathbf{D}_S - \mathbf{e}_S)}{\sigma_1(\mathbf{D})^{2j}} \right)^2 \right] \\ &= \mathbb{E} \left[\frac{1}{\sigma_1(\mathbf{D})^{2j}} \right] \mathbb{E} \left[\left(\sum_{S \in \binom{N \setminus v}{j-1}} \sigma_j(\mathbf{D}_S) \sigma_j(\mathbf{D}_S - \mathbf{e}_S) \right)^2 \right] \\ &\doteq \frac{1}{(n\mu)^{2j}} \mathbb{E} \left[\left(\sum_{S \in \binom{N \setminus v}{j-1}} \sigma_j(\mathbf{D}_S) \sigma_j(\mathbf{D}_S - \mathbf{e}_S) \right)^2 \right]. \end{aligned}$$

We now compute the remaining expectation:

$$\mathbb{E} \left[\left(\sum_{S \in \binom{N \setminus v}{j-1}} \sigma_j(\mathbf{D}_S) \sigma_j(\mathbf{D}_S - \mathbf{e}_S) \right)^2 \right] = \mathbb{E} \left[\sum_{S, T \in \binom{N \setminus v}{j-1}} \sigma_j(\mathbf{D}_S) \sigma_j(\mathbf{D}_S - \mathbf{e}_S) \sigma_j(\mathbf{D}_T) \sigma_j(\mathbf{D}_T - \mathbf{e}_T) \right].$$

Instead of evaluating the expectation explicitly, it suffices to count terms. There are $\binom{n-1}{j-1}^2 \cong \frac{(n-1)^{2j-2}}{(j-1)!}$ of them. Since D has finite fourth moment, the argument of the expectation is bounded by $C(D) \frac{(n-1)^{2j-2}}{(j-1)!}$ for some constant $C(D)$ that depends only on the moments of D . In particular, we obtain that, for any j ,

$$\mathbb{E} \left[\left(q_j(\mathbf{D}) - q_j(\mathbf{D}^{(v)}) \right)^2 \right] = \frac{O(n^{2j-2})}{n^{2j}} = O(n^{-2}).$$

The Efron-Stein inequality now states that

$$\text{var}(q_j(\mathbf{D})) \leq \frac{1}{2} \sum_{v \in N} O(n^{-2}) = O(n^{-1}) .$$

Finally, we complete the proof by applying Chebyshev's inequality. Let \hat{q}_j be the approximation provided by Theorem 3, and recall that $\hat{q}_j(\mathbf{D}) = O(n^{-j})$. Then,

$$\begin{aligned} \mathbb{P}(|\hat{q}_j - q_j(D)| > \epsilon) &= \frac{\text{var}(q_j(\mathbf{D}))}{\epsilon^2} \\ &= \frac{O(n^{-1})}{\epsilon^2} \\ &\rightarrow 0 \end{aligned}$$

as n grows large, completing the proof. □